Supplementary Materials:

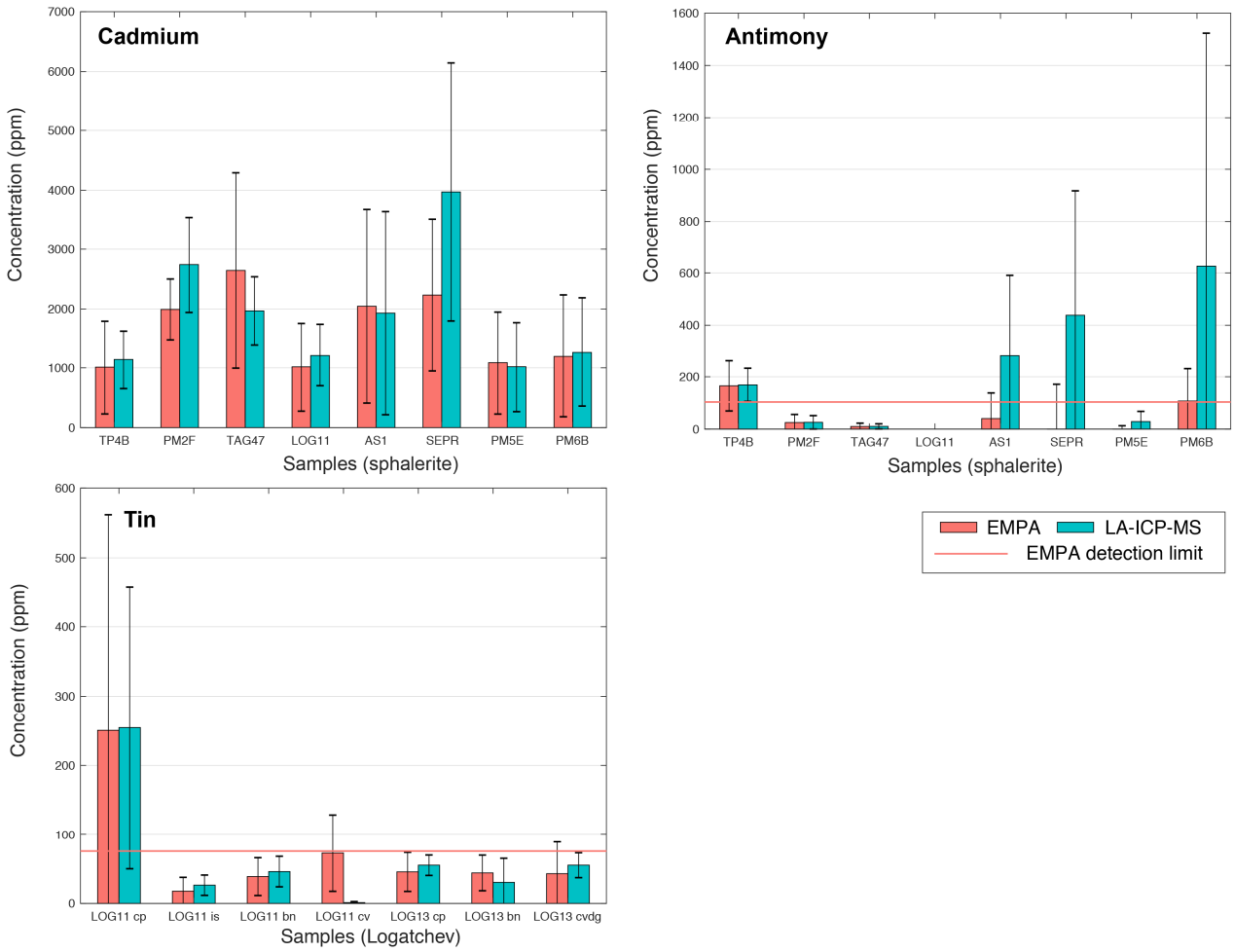

Figure S1. EMPA and LA-ICP-MS results of sphalerite with high concentrations of Cd, Sb and Sn (where concentrations are high enough to exceed EMPA detection limits; shown as horizontal line).

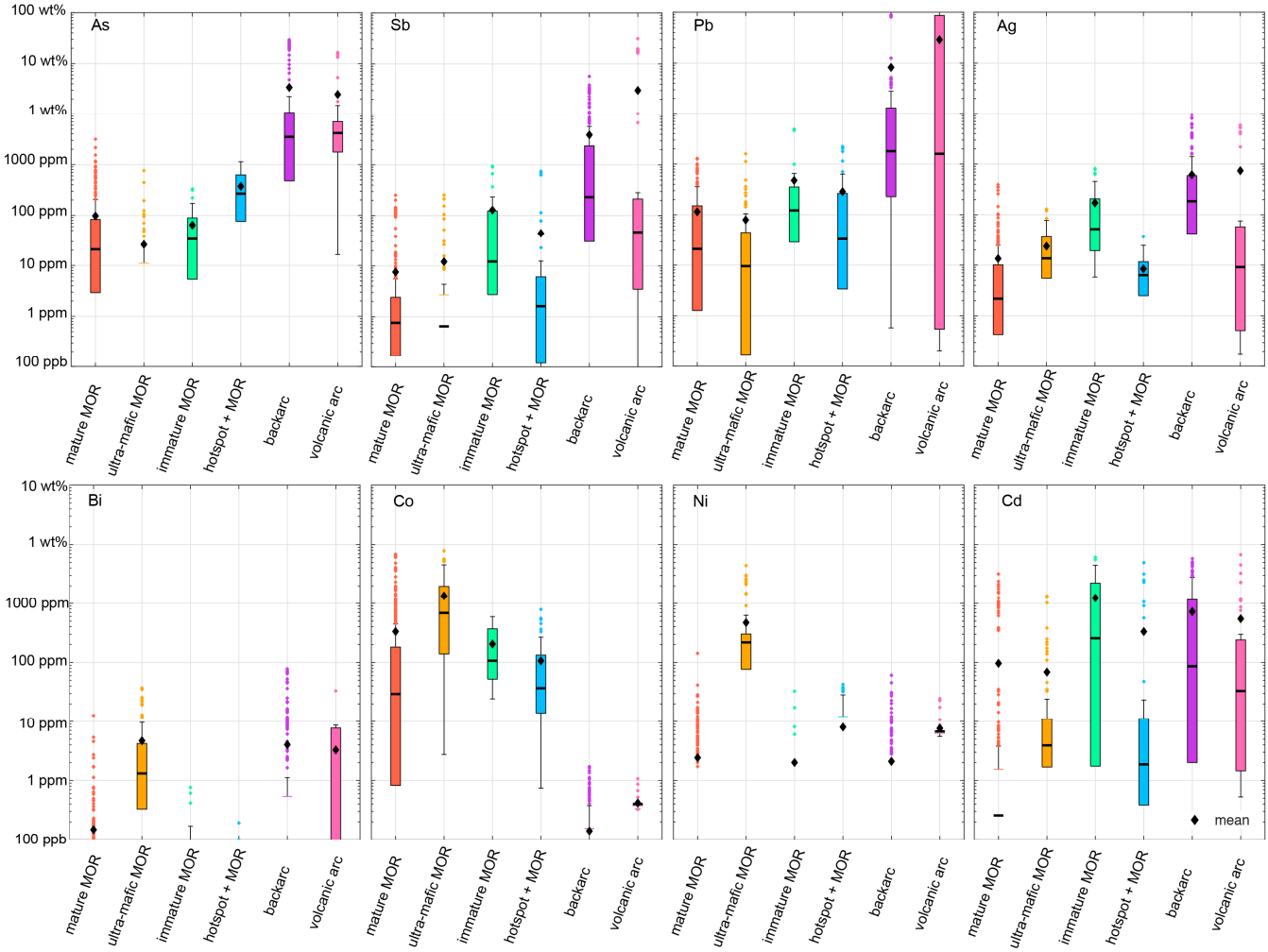

Figure S2. LA-ICP-MS dataset for trace As, Sb, Pb, Ag, Bi, Co, Ni and Cd in all sulfide minerals analysed as a function of geological setting. This excludes tennantite-tetrahedrite and galena, as they are the principal carriers of As, Sb and Pb. Also excluded are sulfides from volcanic arc settings (Palinuro) where only EMPA data was available, which does not include these elements (Ag, Bi, Co, Ni, Cd).

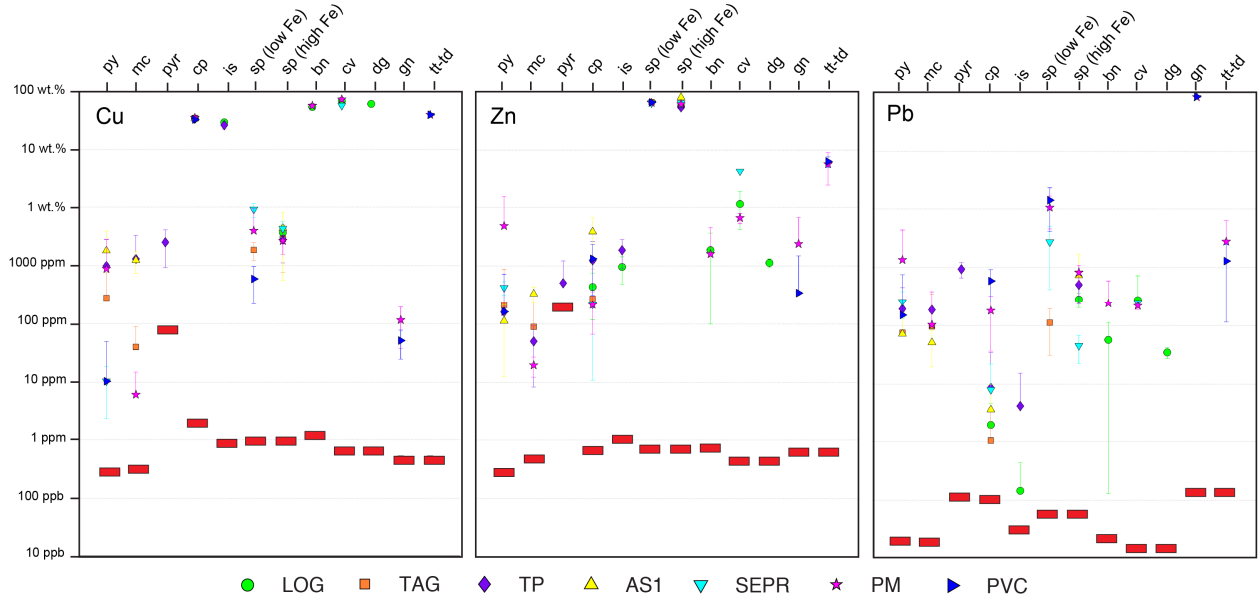

Figure S3. Mean trace element concentrations (Cu, Zn and Pb) in sulfide minerals from all hydrothermal vent sites investigated in this study (based on 625 LA-ICP-MS spot analyses). Also included in this figure are 111 EMPA trace element concentrations of Cu, Zn, Pb, As and Sb where LA-ICP-MS data was unavailable or limited (see text for

discussion). Error bars indicate standard deviation around the arithmetic average. The red bars represent the arithmetic average of LA-ICP-MS detection limit of each element for each mineral phase. Data that is below the detection limit is shown for added clarity for the reader, where confidence levels for values below detection limits is less than 99.9%. Abbreviations of hydrothermal sites used in this figure include LOG (*Logatchev*), TAG (*Trans-Atlantic Geotraverse*), TP (*Turtle Pits*), AS1 (*Axial Seamount*), SEPR (*South East Pacific Rise*), PM (*Pacmanus*) and PVC (*Palinuro*). Abbreviations of minerals used in this figure include py (pyrite), c.py (colloform pyrite), mc (marcasite), c.mc (*colloform marcasite*), pyr (*pyrrhotite*), ccp (*chalcopyrite*), is (i*socubanite*), sp (s*phalerite*), bn (*bornite*), cv (*covellite*), dg (*digenite*), gn (*galena*), tt-td (*tennantite-tetrahedrite*).

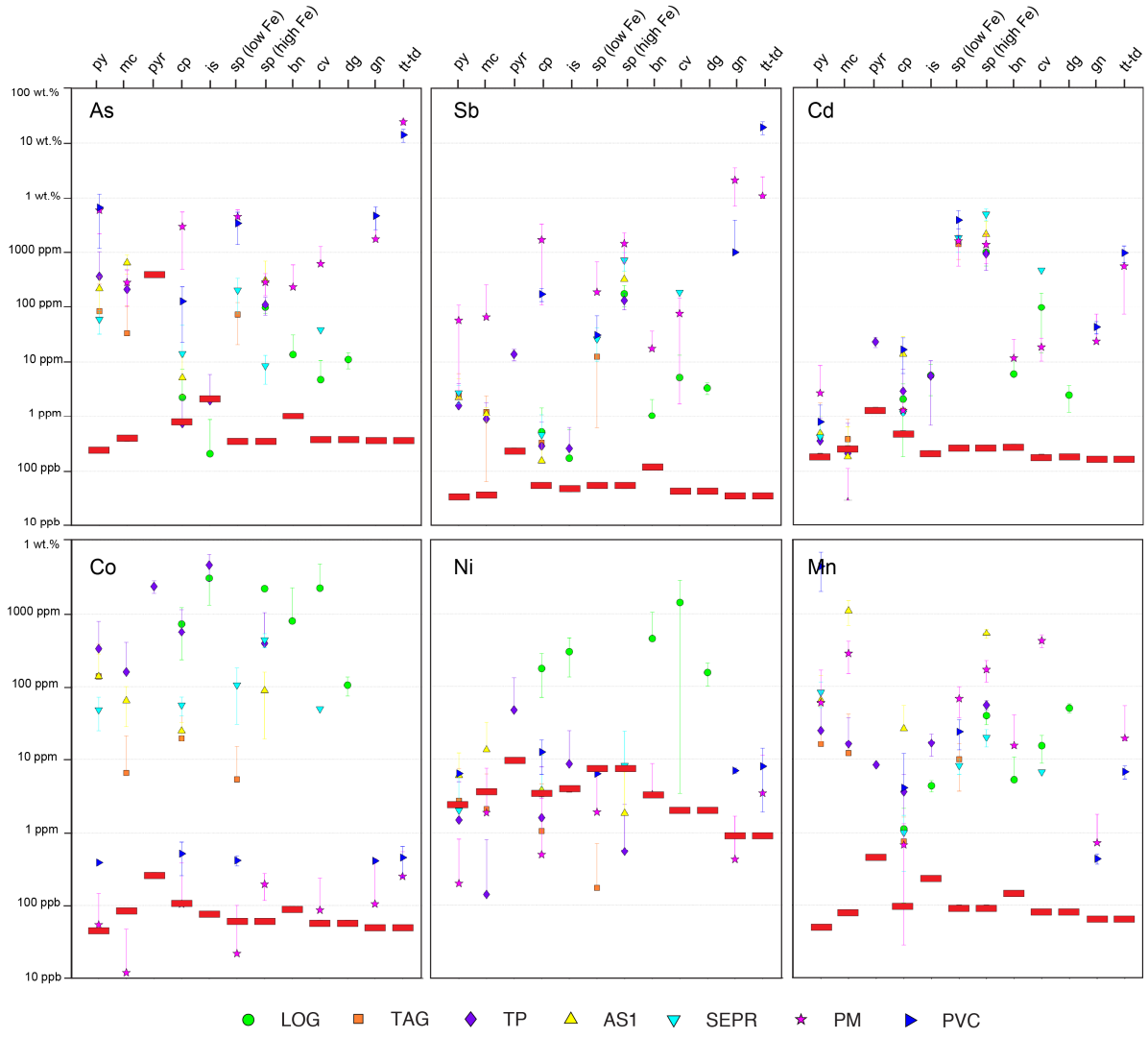

Figure S4. Mean trace element concentrations (As, Sb, Cd, Co, Ni, Mn) in sulfide minerals from all hydrothermal vent sites investigated in this study (based on 625 LA-ICP-MS spot analyses). Also included in this figure are 111 EMPA trace element concentrations of Cu, Zn, Pb, As and Sb where LA-ICP-MS data was unavailable or limited (see text for discussion). Error bars indicate standard deviation around the arithmetic average. The red bars represent the arithmetic average of LA-ICP-MS detection limit of each element for each mineral phase. Data that is below the detection limit is shown for added clarity for the reader, where confidence levels for values below detection limits is less than 99.9%. Abbreviations of hydrothermal sites used in this figure include LOG (*Logatchev*), TAG (*Trans-Atlantic Geotraverse*), TP (*Turtle Pits*), AS1 (*Axial Seamount*), SEPR (*South East Pacific Rise*), PM (*Pacmanus*) and PVC (*Palinuro*). Abbreviations of minerals used in this figure include py (pyrite), c.py (colloform pyrite), mc (marcasite), c.mc (*colloform marcasite*), pyr (*pyrrhotite*), ccp (*chalcopyrite*), is (i*socubanite*), sp (s*phalerite*), bn (*bornite*), cv (*covellite*), dg (*digenite*), gn (*galena*), tt-td (*tennantite-tetrahedrite*).

Table S1: Electron microprobe analysis set up parameters. Background count times are always half of the peak count time. All calibration was performed with a beam current of 10 nA.

Set Up	Beam Current (nA)	Spot Size (μm)	Element	Line	Spectrometer	Crystal	Peak	Bg – ve Offset	Bg +ve Offset	Peak Count Time (s)	Average Detection Limit (ppm)
1) All sulfide minerals (excluding galena & sulfosalts)	150	5	Fe	Kα	5	LLIF	48083	1000	1000	30	197
			S	Kα	2	PET	61430	600	800	20	176
			Pb[1]	Lα	3	LLIF	29155	800	800	60	275
			As[1]	Kα	5	LLIF	29226	800	800	60	172
			Cu	Kα	4	LIF	38250	400	1000	100	148
			Zn	Kα	3	LLIF	35631	500	800	30	62
			Sb	Lα	1	LPET	39306	500	250	60	85
2) Specific As/Pb analyses (sulfosalts and As/Pb in minerals where no LA-ICP-MS data was obtained (pyrrhotite in TP4B and fine-grained colloform pyrite and chalcopyrite in Pacmanus samples)	150	1	Fe	Kα	5	LLIF	48083	1000	1000	30	115
			S	Kα	2	PET	61430	600	800	20	181
			Pb	Lβ	3	LLIF	24386	600	600	60	574
			As	Lα	4	TAP	37639	600	500	180	72
			Cu	Kα	5	LLIF	38250	400	1000	30	230
			Zn	Kα	3	LLIF	35631	500	800	20	91
			Sb	Lα	1	LPET	39306	500	250	60	81
			Mn	Kα	5	LLIF	52205	1000	800	30	86
			Co	Kα	3	LLIF	44427	200	200	30	71
3) Hg analyses (chalcopyrite and tennantite-tetrahedrite	150	1	Fe	Kα	4	LIF	48083	1000	1000	30	270
			S	Kα	2	PET	61430	600	800	20	191

[1] Analyses of Pb Lα and As Kα interfere with each other and were not used during trace element studies. Where Pb and As analyses were important (in minerals/samples where no LA-ICP-MS data was obtained), they were undertaken again using a specific set up to avoid interferences outlined in Table S2. Where Pb analyses were important for galena (use as internal standard for LA-ICP-MS data), they were analysed again, combined with further analyses of Hg, outlined in Table S6.

Set Up	Beam Current (nA)	Spot Size (μm)	Element	Line	Spectrometer	Crystal	Peak	Bg – ve Offset	Bg +ve Offset	Peak Count Time (s)	Average Detection Limit (ppm)
(excluding PVC)			As[1]	Kα	5	LLIF	37639	800	800	60	325
			Cu	Kα	4	LIF	38250	400	1000	30	447
			Zn	Kα	5	LLIF	35631	500	800	60	142
			Sb	Lα	2	PET	39306	500	250	120	124
			Hg	Mα	1	LPET	64448	800	500	150	92
			Hg	Mα	3	LPET	64448	800	500	150	92
4) Hg in pyrite and pyrrhotite (excluding PVC)	150	1	Fe	Kα	4	LIF	48083	1000	1000	30	125
			S	Kα	2	PET	61430	600	800	20	201
			As[1]	Kα	5	LLIF	37639	800	800	80	275
			Cu	Kα	4	LIF	38250	400	1000	90	117
			Zn	Kα	5	LLIF	35631	500	800	60	550
			Sb	Lα	2	PET	39306	500	250	120	130
			Hg	Mα	1	LPET	64448	800	500	150	100
			Hg	Mα	3	LPET	64448	800	500	150	100
5) Hg in sphalerite (excluding PVC)	150	1	Fe	Kα	4	LIF	48083	1000	1000	120	129
			S	Kα	2	PET	61430	600	800	20	196

Set Up	Beam Current (nA)	Spot Size (μm)	Element	Line	Spectrometer	Crystal	Peak	Bg – ve Offset	Bg +ve Offset	Peak Count Time (s)	Average Detection Limit (ppm)
			As[1]	Kα	5	LLIF	37639	800	800	90	271
			Cu	Kα	5	LLIF	38250	400	1000	60	145
			Zn	Kα	4	LIF	35631	500	800	30	533
			Sb	Lα	2	PET	39306	500	250	120	128
			Hg	Mα	1	LPET	64448	800	500	150	96
			Hg	Mα	3	LPET	64448	800	500	150	96
6) Pb and Hg in galena (to avoid interferences)	200	1	Fe	Kα	5	LLIF	48083	500	400	60	50
			S	Kα	2	PET	61430	600	800	20	160
			Pb	Lβ	4	LIF	29154	800	800	30	1607
			As	Lα	4	LTAP	37639	600	500	400	29
			Cu	Kα	5	LLIF	38250	400	1000	130	69
			Zn	Kα	5	LLIF	35631	500	800	130	67
			Sb	Lα	2	PET	39306	500	250	300	82
			Hg	Mα	3	LPET	64448	800	2000	200	100
7) Hg in PVC tennantite-tetrahedrite DS4 slit setting	50 (to avoid dead time for Cu)	5	Fe	Kα	5	LLIF	48083	1000	1000	120	75
			S	Kα	2	PET	61430	600	800	20	302

Set Up	Beam Current (nA)	Spot Size (μm)	Element	Line	Spectrometer	Crystal	Peak	Bg – ve Offset	Bg +ve Offset	Peak Count Time (s)	Average Detection Limit (ppm)
Differential auto mode			Pb	Lβ	5	LLIF	24375	800	800	130	1071
			As	Lα	4	LTAP	37639	600	500	400	101
			Cu	Kα	5	LLIF	38250	400	1000	130	212
			Zn	Kα	4	LIF	35631	500	800	30	605
			Sb	Lα	2	PET	39306	500	250	300	191
			Hg	Mα	3	LPET	64448	800		400	287
8) Hg in PVC and PM5E sphalerite	100 (to avoid dead time for Zn)	5	Fe	Kα	5	LLIF	48083	1000	1000	120	35
			S	Kα	2	PET	61430	600	800	20	170
			Pb	Lβ	5	LLIF	24375	600	600	130	530
			As	Lα	1	LTAP	37639	600	500	400	33
			Cu	Kα	5	LLIF	38250	400	1000	130	46
			Zn	Kα	4	LIF	35631	500	800	30	316
			Sb	Lα	2	PET	39306	500	250	300	62
			Hg	Mα	3	LPET	64448	800	500	400	110
9) Hg in PVC pyrite	200	1	Fe	Kα	5	LLIF	48083	1000	1000	120	103
			S	Kα	2	PET	61430	600	800	20	163

Set Up	Beam Current (nA)	Spot Size (μm)	Element	Line	Spectrometer	Crystal	Peak	Bg – ve Offset	Bg +ve Offset	Peak Count Time (s)	Average Detection Limit (ppm)
			Pb	Lβ	5	LLIF	24375	600	600	130	486
			As	Lα	1	LTAP	37639	600	500	400	24
			Cu	Kα	5	LLIF	38250	400	1000	130	45
			Zn	Kα	4	LIF	35631	500	800	30	272
			Sb	Lα	2	PET	39306	500	250	300	59
			Hg	Mα	3	LPET	64448	800	2000	400	90

Table S2: Comparison of measured concentrations (calculated using NISTSRM610 as the external standard, with no normalisation using an internal standard (100 wt.% normalisation) of the same elements from different reference materials versus their published or communicated values, after 3 sigma outlier elimination. *(*information value*).

SRM	Reference	Published values and pers. commun.													Measured values												N
		Fe	Cu	Pb	Zn	As	Ni	Mn	Co	Ag	Cd	Sn	Sb	Bi	Fe	Cu	Pb	Zn	As	Ni	Mn	Co	Ag	Cd	Sn	Sb	Bi	
GOR132-G	GeoReM preferred values 03/2011	78508 ± 777	205 ± 21	19.5 ± 1.7	76.8 ± 12.5	(0.2)*	1187 ± 58	1192.7 ± 54.2	92.7 ± 5.7	0.04	0.08	0.34 ± 0.09	0.06 ± 0.04	0.0107 ± 0.003	78940 ± 2304	221 ± 7.2	19.7 ± 1.3	77.6 ± 5.7	0.33 ± 0.91	1240 ± 34.6	1188 ± 27.4	97.6 ± 2.5	0.08 ± 0.07	0.36 ± 0.61	0.28 ± 0.13	0.12 ± 0.14	0.04 ± 0.06	136-150
KL2-G	GeoReM preferred values 03/2011	83172 ± 777	87.9 ± 9.1	2.1 ± 0.1	110 ± 10	(0.2)*	112 ± 5	1277.9 ± 69.7	41.2 ± 2.3	0.15	0.09	1.54 ± 0.29	0.14 ± 0.03	0.04 ± 0.014	83347 ± 1676	93.7 ± 3.3	1.9 ± 0.3	115.7 ± 7.9	0.14 ± 1.2	112.2 ± 6.7	1298 ± 17.5	43.3 ± 1.2	0.09 ± 0.09	0.00 ± 0.42	1.31 ± 0.32	0.2 ± 0.13	0.04 ± 0.04	31-34
StHs6-80-G	GeoReM preferred values 03/2011	33968 ± 544	41.5 ± 8.3	10.3 ± 0.9	67 ± 7	2.73 ± 0.48	23.7 ± 3.8	588.6 ± 31	13.2 ± 1.1	0.02	0.10	1.10 ± 0.2	0.20 ± 0.07	0.11 ± 0.07	33122 ± 824	39.9 ± 2.6	10.3 ± 0.7	64.9 ± 5.9	2.4 ± 0.86	21.8 ± 4.9	568.9 ± 12.5	12.8 ± 0.5	0.03 ± 0.05	0.10 ± 0.29	0.72 ± 0.26	0.21 ± 0.11	0.09 ± 0.03	18-20
T1-G	GeoReM preferred values 03/2011	50059 ± 466	18.8 ± 2	11.6 ± 1.5	74 ± 10	0.96 ± 0.44	10.6 ± 1.3	983.6 ± 46.5	18.9 ± 0.8	0.10	0.20	2.00 ± 0.5	0.25 ± 0.05	0.10 ± 0.05	48421 ± 1810	19.9 ± 1.2	9.8 ± 0.7	72.7 ± 4.1	1.00 ± 0.98	10.3 ± 2.5	1005.9 ± 34.1	18.6 ± 0.8	0.03 ± 0.06	0.52 ± 0.67	1.55 ± 0.21	0.36 ± 0.14	0.10 ± 0.05	68-75

Table S3: Comparison of measurements between LA-ICP-MS (prior to normalisation with EMPA measurements) and EMPA data for trace elements that are in high enough concentration to be detected by both techniques (Cd, Sb, Co, Ni). No comparison of As and Pb can be made between EMPA and LA-ICP-MS measurements due to the interference of the lines chosen for respective elements during EMPA. Concentrations of Ag, Sn and Bi are generally below detection limits for EMPA, making comparison impossible. Standard deviations (SD) around the mean value are also presented. SD is always higher than the associated error on the measurement.

Sample	Mineral	Mean concentration (LA-ICP-MS)									Mean concentration (EMPA)								
		Co	SD	Ni	SD	Cd	SD	Sb	SD	N	Co	SD	Ni	SD	Cd	SD	Sb	SD	N
Cu phases: Co, Ni from high-T, ultra-mafic hosted sites																			
LOG11	cp	1037	404	257	37					21	1015	371	215	61					13
LOG13	cp	182	5	24	5					7	161	58	bdl						13
LOG11	is	3852	734	351	121					8	5037	1002	409	100					21
LOG11	bn	1490	1805	796	660					9	685	1138	332	640					25
LOG13	bn	23	19	46	51					8	bdl		bdl						11
LOG11	cc-cv-dg	4390	2021	2655	989					8	3565	2764	871	1149					38

LOG13	cc-cv-dg	105	46	173	77					8	bdl		bdl					11
TP4B	cp	948	442	bdl						8	723	205	bdl					28
TP4B	is	4677	1862	bdl						8	3729	1752	bdl					24
Zn phases from all sites: Cd, Sb																		
TAG47	sp					1967	571	10	10	7					2643	1648	bdl	7
TAGH	sp					784	318	24	19	3					522	346	bdl	20
LOG11	sp	2706	242	bdl		1222	520	216	87	4	2791	921			1230	627	n/a	19
TP4B high Fe	sp	43	20	bdl		1168	637	157	34	8	bdl		bdl		1012	782	163 96	25
SEPR	sp					3972	2173	439	479	8					2231	1284	bdl	73
AS1	sp					1930	1713	284	307	7					2045	1634	bdl	13
PM2D2	sp					1825	485	1816	829	5					n/a		1747 2203	23
PM5ETS low Fe	sp					1018	751	29	39	8					973	726	n/a	23
PM6BTS low Fe	sp					1274	913	626	897	9					1208	1026	108 124	30
PM2FTS low Fe	sp					2741	802	26	26	5					1992	509	25 31	29

Table S4. Powder X-ray Diffraction (XRD) set up parameters for sample powders.

Anode material	Cu	**Generator voltage (kV)**	40	Start θ	10
K-Alpha1	1.540598	**Tube current (mA)**	30	End θ	80
K-Alpha2	1.544426	**Fixed Divergence slit (°)**	0.5	Step size (θ)	0.02
Ratio K-Alpha2/K-Alpha1	0.5	**Antiscatter slit (°)**	0.5	Time step (s)	10
Scan axis	2 Theta-Omega	**Receiving height (mm)**	0.5	No. of points	3500

Table S5. Major element composition of sulfide minerals from EMPA in wt% and 2 sigma standard deviation. N; number of analysis, bdl; below the minimum detection limit, cp (chalcopyrite), py (pyrite), mc (marcasite), is (isocubanite), sp (sphalerite), pyr (pyrrhotite), cv (covellite), cc (chalcocite), bn (bornite), tt-td (tennantite-tetrahedrite), gn (galena)

Sample	Mineral		S		Fe		Cu		Zn		Total
		N	mean	SD	mean	SD	mean	SD	mean	SD	mean
TAG-1 (Central), TAG hydrothermal vent field, Mid-Atlantic Ridge											
TAGM	cp	10.0	35.7	0.8	30.2	1.7	34.7	3.0	Bdl	Bdl	100.6
TAGM	py	12.0	53.6	1.2	46.3	2.6	0.0	0.0	Bdl	Bdl	99.9
TAGM	mc	10.0	53.6	1.3	46.3	2.6	0.0	0.0	Bdl	Bdl	10bdl
TAG6F	cp	6.0	34.7	1.1	30.6	1.4	34.9	1.4	Bdl	Bdl	100.3
TAG6F	py	10.0	52.6	1.7	46.4	2.1	0.0	0.0	Bdl	Bdl	99.1
TAG6F colloform interior	py	2.0	53.2	1.7	46.4	2.1	Bdl	Bdl	Bdl	Bdl	99.6
TAG6F colloform exterior	py	2.0	53.0	1.7	46.2	2.1	Bdl	Bdl	Bdl	Bdl	99.2
TAG27	cp	9.0	35.0	1.1	30.3	1.4	34.8	1.4	Bdl	Bdl	100.1
TAG27	py	4.0	51.8	1.6	46.1	2.1	0.0	0.0	Bdl	Bdl	98.0
TAG-4 (West), TAG hydrothermal vent field, Mid-Atlantic Ridge											
TAG46	cp	9.0	35.1	1.1	30.1	1.4	34.8	1.4	Bdl	Bdl	100.1
TAG46	sp	2.0	34.2	1.2	8.2	0.4	0.4	0.0	58.5	0.8	101.5
TAG46	py	11.0	51.9	1.7	46.3	2.1	0.0	0.0	0.0	0.0	98.3
TAG46	mc	12.0	52.0	1.7	46.2	2.1	Bdl	Bdl	0.0	0.0	98.2
TAGJ	cp	21.0	35.1	0.9	30.0	1.6	34.6	2.3	Bdl	Bdl	99.8
TAGJ	py	13.0	53.0	1.3	46.2	2.4	0.1	0.0	Bdl	Bdl	99.4
TAGJ	mc	14.0	52.5	1.3	46.3	2.6	0.1	0.0	0.0	0.0	99.0
TAG47	sp	3.0	33.7	1.2	1.1	0.1	0.2	0.0	65.7	0.9	101.1
TAG47	py	9.0	53.1	1.7	46.2	2.1	Bdl	Bdl	0.0	0.0	99.4
TAG47	mc	9.0	52.7	1.7	46.1	2.1	Bdl	Bdl	0.0	0.0	98.9
TAG48	sp	6.0	33.7	1.2	2.4	0.1	0.5	0.0	63.5	0.9	101.2
TAG48	py	9.0	52.5	1.7	45.8	2.1	0.0	0.0	0.0	0.0	98.5
TAG48 colloform interior	py	5.0	51.9	1.7	45.8	2.1	Bdl	Bdl	0.0	0.0	97.7
TAG48 colloform exterior	py	5.0	52.3	1.7	44.4	2.0	0.2	0.0	0.0	0.0	97.0
TAG48	mc	10.0	52.7	1.7	45.9	2.1	Bdl	Bdl	0.0	0.0	98.7
TAG48 colloform	mc	2.0	52.5	1.7	45.5	2.1	Bdl	Bdl	Bdl	Bdl	98.1
TAGH	sp	27.0	33.5	0.9	2.0	0.1	0.2	0.0	64.8	1.1	100.4
TAGH	py	22.0	53.2	1.3	46.4	2.4	Bdl	Bdl	0.0	0.0	99.6
TAGH	mc	14.0	52.7	1.4	46.4	2.6	Bdl	Bdl	0.1	0.0	99.2
TAGI	py	13.0	52.6	1.2	45.9	2.4	Bdl	Bdl	Bdl	Bdl	98.5
TAGI colloform	py	8.0	50.0	1.2	44.4	2.5	Bdl	Bdl	Bdl	Bdl	94.5
TAGI	mc	13.0	51.7	1.4	45.9	2.6	Bdl	Bdl	0.0	0.0	97.7
TAG-5 (North), TAG hydrothermal vent field, Mid-Atlantic Ridge											
TAGK	cp	17.0	35.2	0.8	29.9	1.5	34.7	2.3	Bdl	Bdl	99.8
TAGK	py	19.0	53.0	1.3	46.4	2.4	0.1	0.0	0.0	0.0	99.6

Sample	Mineral		S		Fe		Cu		Zn		Total
		N	mean	SD	mean	SD	mean	SD	mean	SD	mean
TAGL	cp	17.0	35.3	0.8	29.9	1.5	34.8	2.3	Bdl	Bdl	100.0
TAGL	py	14.0	53.2	1.3	46.5	2.4	0.1	0.0	Bdl	Bdl	99.8
Inactive mound, Turtle Pits hydrothermal vent field, Mid-Atlantic Ridge											
TP2L	cp	9.0	35.4	0.9	30.5	1.6	34.3	2.1	Bdl	Bdl	100.1
TP2L	py	9.0	52.8	1.2	46.0	2.3	0.1	0.0	Bdl	Bdl	99.0
TP2LTS colloform	py	3.0	52.3	1.2	44.5	2.5	0.3	0.0	0.0	0.0	97.1
TP2LTS	mc	10.0	53.2	0.2	46.0	0.0	0.1	0.0	Bdl	Bdl	99.4
Southern Tower, Turtle Pits hydrothermal vent field, Mid-Atlantic Ridge											
TP4B	cp	30.0	35.7	1.1	31.5	1.7	33.0	2.1	0.1	0.0	100.4
TP4B	is	26.0	36.1	1.0	38.9	2.0	23.9	1.4	0.1	0.0	99.4
TP4BTS	is	4.0	34.7	0.2	40.4	0.0	22.1	0.0	Bdl	Bdl	97.3
TP4BTS	sp	9.0	33.3	0.2	12.2	0.0	1.0	0.0	52.0	0.1	98.7
TP4B	sp	25.0	34.2	0.9	11.5	1.7	0.4	0.0	54.4	1.0	100.5
TP4B	py	36.0	53.2	1.5	46.4	2.4	0.1	0.0	0.0	0.0	99.8
TP4B	mc	11.0	53.5	1.5	46.1	2.6	0.1	0.0	0.2	0.0	100.0
TP4BTS	mc	22.0	52.8	0.2	46.3	0.1	0.1	bdl	0.0	0.0	99.3
TP4BTS	pyr	26.0	38.4	0.2	59.6	0.1	0.4	0.0	0.1	0.0	98.8
TP4B	pyr	14.0	38.8	1.1	56.5	3.1	0.3	0.0	0.1	0.0	96.6
Irina 1, Logatchev-1 hydrothermal vent field, Mid-Atlantic Ridge											
LOG13	cp	13.0	35.4	0.8	29.7	1.5	34.8	2.4	Bdl	Bdl	100.0
LOG13	sp	18.0	32.1	0.2	1.6	0.0	2.3	0.0	60.4	0.1	97.5
LOG13	cp(bn)	11.0	30.4	0.9	18.0	1.0	42.1	3.0	0.0	0.0	90.8
LOG13TS	cv(bn)	11.0	30.0	0.9	8.6	0.6	58.6	3.9	bdl	bdl	97.3
Candelaber, Logatchev-1 hydrothermal vent field, Mid-Atlantic Ridge											
LOG11	cp	13.0	35.6	0.9	30.8	1.7	33.7	2.4	0.0	0.0	100.2
LOG11TS	is	23.0	36.0	1.2	40.3	1.8	24.4	1.0	Bdl	Bdl	100.8
LOG11	is	21.0	35.7	1.0	38.8	2.1	24.4	1.5	0.1	0.0	99.5
LOG11	sp	19.0	33.4	0.2	8.9	0.0	0.5	0.0	55.7	0.1	98.8
LOG11TS	bn(cp)	25.0	32.6	1.0	14.3	0.7	54.5	2.2	0.0	0.0	101.6
LOG11TS	cv-pore spaces	28.0	32.7	0.2	2.6	0.0	49.0	0.1	0.9	0.0	85.9
16°43'S hydrothermal vent field, East Pacific Rise											
SEPR	cp	22.0	35.6	0.9	30.6	1.5	34.3	2.1	0.1	0.0	100.6
SEPRTS	cp	10.0	36.1	0.4	31.2	0.3	34.4	0.3	0.0	0.0	101.7
SEPR	sp	2.0	34.0	0.8	4.3	0.2	0.6	0.1	60.7	0.9	100.0
SEPRTS	sp	73.0	32.6	0.5	1.0	0.0	1.4	0.0	63.3	0.4	99.4
SEPR	py	16.0	53.4	1.4	46.2	2.6	0.3	0.0	0.1	0.0	10bdl
SEPRTS	py	7.0	53.9	0.6	46.5	0.4	0.3	0.0	0.1	0.0	100.9
SEPR	bn-sp	14.0	30.1	0.8	7.6	0.5	53.0	4.2	1.2	0.0	92.4
*Ashes hydrothermal vent field, Juan de Fuca Ridge**											
AS1	cp	19.0	35.3	0.9	31.1	1.6	33.8	2.3	0.2	0.0	100.3
AS1	sp	13.0	33.8	0.9	11.2	2.0	3.9	0.3	51.2	1.1	100.3

Sample	Mineral		S		Fe		Cu		Zn		Total
		N	mean	SD	mean	SD	mean	SD	mean	SD	mean
AS1	py	26.0	52.8	1.3	46.1	2.5	0.1	0.0	0.8	0.0	100.1
AS1 colloform	py	30.0	52.5	1.4	45.6	2.5	0.4	0.0	0.0	0.0	98.7
AS1 colloform interior	mc	7.0	53.0	1.2	46.4	2.6	0.1	0.0	0.0	0.0	99.7
AS1 colloform exterior	mc	6.0	53.3	1.2	45.7	2.5	0.2	0.0	0.0	0.0	99.6
Roman Ruins, Pacmanus hydrothermal vent field, Pacmanus Basin, Papua New Guinea											
PM2D	sp	23.0	33.6	0.9	5.9	0.3	0.3	0.0	60.5	1.1	100.6
PM2D	py	36.0	52.7	1.3	46.4	2.3	Bdl	Bdl	0.0	0.0	99.9
PM2D	mc	12.0	53.4	1.4	46.3	2.6	Bdl	Bdl	0.0	0.0	100.2
Satanic Mills, Pacmanus hydrothermal vent field, Pacmanus Basin, Papua New Guinea											
PM5E	cp	30.0	35.5	0.8	30.0	1.4	34.9	2.0	0.0	0.0	100.8
PM5E	sp	3.0	32.9	0.8	2.2	0.1	2.2	0.2	60.2	0.9	100.0
PM5ETS	sp	23.0	32.8	0.2	0.5	0.0	0.4	0.0	64.2	0.1	99.3
PM5E colloform	py	9.0	51.6	1.6	41.6	1.9	0.7	4.2	1.8	0.0	97.5
PM5E	mc	19.0	53.6	1.3	46.4	2.6	0.1	0.0	0.0	0.0	100.3
PM5E	tt-td	51.0	25.1	0.7	6.0	0.3	40.7	2.1	4.0	0.1	100.8
PM6B	cp	19.0	35.6	0.9	29.9	1.4	34.3	1.1	0.3	0.0	100.2
PM6B high Fe	sp	25.0	33.2	0.9	1.6	0.1	0.2	0.0	64.2	1.3	102.4
PM6B	sp	30.0	33.2	1.0	0.7	0.1	0.1	0.0	63.7	1.4	102.6
PM6B	py	24.0	51.2	1.4	42.8	2.2	0.4	0.0	1.1	0.0	98.3
PM6B colloform	py	10.0	51.6	1.6	42.9	1.9	0.5	0.0	1.2	0.0	98.2
PM6B	tt-td	9.0	26.6	0.8	2.5	0.1	39.7	1.3	8.5	0.1	100.1
Solwara-8, Pacmanus hydrothermal vent field, Pacmanus Basin, Papua New Guinea											
PM2F	cp	25.0	35.5	0.9	29.6	1.5	35.3	2.4	0.1	0.0	101.2
PM2F low Fe	sp	29.0	33.4	0.9	0.5	0.0	1.6	0.2	64.6	1.0	107.0
PM2F high Fe	sp	3.0	32.7	1.1	1.5	0.1	3.6	0.2	58.9	1.4	100.0
PM2F	tt-td	25.0	20.0	0.6	5.5	0.3	40.2	2.7	5.5	0.1	92.9
PM2F	bn	9.0	28.0	0.7	7.0	0.4	63.3	5.1	0.4	0.0	99.6
PM2F2	cv	10.0	28.5	0.7	3.9	0.2	69.1	5.9	0.1	0.0	101.8
Palinuro Volcanic Complex, Aeolian Island Arc, Italy											
PVC851	sp	7.0	33.4	0.8	0.3	0.0	0.1	0.0	64.9	0.7	101.5
PVC932	py	6.0	54.9	1.2	44.2	0.6	Bdl	Bdl	Bdl	Bdl	100.0
PVC932	tt-td	6.0	26.9	0.6	3.5	0.1	39.4	0.3	4.0	0.1	100.0
			S		Fe		Pb		Zn		Total
Sample		N	mean	SD	mean	SD	mean	SD	mean	SD	mean
Satanic Mills, Pacmanus hydrothermal vent field, Pacmanus Basin, Papua New Guinea											
PM2D	gn	5.0	13.9	0.3	0.1	0.0	84.3	0.8	0.6	0.0	100.6
PM2D Hg*	gn	19.0	13.6	0.3	0.1	bdl	83.7	0.8	1.1	0.0	100.0
Roman Ruins, Pacmanus hydrothermal vent field, Pacmanus Basin, Papua New Guinea											
PM6B Hg*	gn	12.0	13.8	0.3	0.0	bdl	86.0	0.8	0.5	0.0	101.3

Sample	Mineral		S		Fe		Cu		Zn		Total
		N	mean	SD	mean	SD	mean	SD	mean	SD	mean
Palinuro Volcanic Complex, Aeolian Island Arc, Italy											
PVC932 Hg*	gn	19.0	13.8	0.3	0.1	bdl	86.4	0.8	0.0	0.0	100.7
PVC851 Hg*	gn	28.0	14.0	0.3	0.0	bdl	84.7	0.8	0.8	0.0	100.8

Table S6 Trace element distributions in a range of sulfide minerals in massive sulfides from LA-ICP-MS in ppm and 1 sigma error. N;number of analysis bdl; below the minimum detection limit

		Ag		As		Bi		Cd		Co		Mn		Ni		Pb		Sb		Cu		Zn		Fe		Hg	
Sample	**N**	**mean**	**SD**	**mean**	**SD**	**mean**	**SD**	**mean**	**SD**	**mean**	**SD**	**mean**	**SD**	**mean**	**SD**	**mean**	**SD**	**mean**	**SD**	**mean**	**SD**	**mean**	**SD**	**mean**	**SD**	**mean**	**SD**
SPHALERITE (90)																											
TAG-4 (West), TAG hydrothermal vent field, Mid-Atlantic Ridge																											
TAG47 porous	7	38.7	5.31	63.3	7.14	Bdl	Bdl	1740	182	Bdl	bdl	10.7	0.808	Bdl	bdl	83	22.1	9.08	1.39	2020	276	657000	84000	6890	1010		
TAGH massive	3	55.9	2.68	93.2	3.43	Bdl	bdl	669	23.1	17.8	0.927	8.12	0.204	Bdl	bdl	181	6.05	20.5	1.31	1470	28.8	648000	16100	6800	261		
Southern Tower, Turtle Pits hydrothermal vent field, Mid-Atlantic Ridge																											
TP4BTS colloform	4	8.19	1.11	129	18.6	Bdl	bdl	892	80.5	1090	44.9	52.1	2.89	Bdl	bdl	332	37.9	146	12.1	3660	646	520000	33800	82600	2910		
TP4B colloform	8	236	16.9	105	6.05	Bdl	bdl	966	46.2	35.3	1.96	57.3	1.71	Bdl	bdl	595	37.6	129	4.92	2360	115	544000	23800	77200	4330		
Candelaber, Logatchev-1 hydrothermal vent field, Mid-Atlantic Ridge																											
LOG11 massive	4	15.1	1.25	98.4	10.2	Bdl	bdl	1010	87.4	2220	139	40	2.37	Bdl	Bdl	284	29.6	178	15.2	3690	209	557000	25200	61800	3400		
16°43'S hydrothermal vent field, East Pacific Rise																											
SEPR colloform	4	252	9.95	207	13.5	Bdl	bdl	1840	84.7	105	3.67	8.12	0.512	bdl	bdl	2730	110	26	1.7	9120	339	633000	25900	5970	319		
SEPR massive	4	15.5	1.8	8.55	3.99	Bdl	bdl	4900	296	430	23.4	20.2	1.91	Bdl	bdl	45.3	7.71	724	53.6	4320	298	633000	25200	27700	1400		
*Ashes hydrothermal vent field, Juan de Fuca Ridge**																											
AS1TS massive	3	2.6	0.359	3.5	1.46	0.0695	0.0346	3080	259	141	10.5	556	40	3.21	4.35	5.67	1.05	51.6	7.58	3050	700	801000	63200	101000	7560		
AS1TS massive	4	12.5	1.26	720	56.4	0.0507	0.0531	850	68.3	18.5	1.71	490	35.9	bdl	bdl	1710	145	690	51.4	6150	458	771000	59600	101000	7610		
Roman Ruins, Pacmanus hydrothermal vent field, Pacmanus Basin, Papua New Guinea																											
PM2D2 colloform	5	486	37.5	273	21.6	bdl	bdl	1650	53.6	0.165	0.0962	182	3.31	bdl	bdl	789	50.4	1630	88.6	3040	126	605000	21000	68100	2640		
PM2D colloform	1	392	14.6	366	17.6	bdl	bdl	87.7	3.08	0.339	0.113	99.7	2.09	bdl	bdl	1020	49.3	520	39.2	794	48.1	605000	12300	29700	979		
Satanic Mills, Pacmanus hydrothermal vent field, Pacmanus Basin, Papua New Guinea																											
PM5E colloform	3	47.4	7.35	2760	135	0.156	0.0679	2730	182	bdl	bdl	38	1.62	bdl	bdl	6190	275	0.534	0.396	644	96.3	602000	27400	1960	146		
PM5E2 colloform	1	52.8	1.73	3070	87.9	bdl	bdl	4700	198	bdl	bdl	44.3	0.968	bdl	bdl	7060	255	19.5	1.82	4570	487	602000	16700	6190	456		
PM5ETS colloform	8	23.2	2.97	4350	258	bdl	bdl	869	75.3	0.0261	0.0795	42.3	1.46	bdl	bdl	9070	544	24.7	5.38	938	203	642000	17900	2480	429		
PM6B TS colloform	9	203	15.8	5820	312	bdl	bdl	1110	86.1	bdl	bdl	99.6	3.35	bdl	bdl	17900	928	553	44.2	923	91.7	637000	20000	4610	279		

Sample	N	Ag		As		Bi		Cd		Co		Mn		Ni		Pb		Sb		Cu		Zn		Fe		Hg	
		mean	SD	mean	SD	mean	SD	mean	SD	mean	SD	mean	SD	mean	SD	mean	SD	mean	SD	mean	SD	mean	SD	mean	SD	mean	SD
PM6B low Fe colloform	3	407	14.9	3410	83.6	bdl	bdl	1790	64.6	bdl	bdl	108	2.33	bdl	bdl	10700	300	451	24.2	1940	113	637000	15000	6760	238		
PM6B2 low fe colloform	3	119	11.8	4740	200	bdl	bdl	953	64.6	0.0236	0.0418	92	2.08	bdl	bdl	14300	653	59	3.47	384	34.8	637000	14900	4950	296		
Solwara-8, Pacmanus hydrothermal vent field, Pacmanus Basin, Papua New Guinea																											
PM2F2 low Fe massive	4	19.8	1.04	3500	187	bdl	bdl	1930	91.9	0.102	0.0787	64	2.61	bdl	bdl	2810	131	11.6	0.79	10200	551	646000	21300	3290	165		
PM2F low Fe massive	5	131	3.18	4510	135	bdl	bdl	2400	133	0.0226	0.0416	38.7	1.21	bdl	bdl	7010	290	22.5	1.08	14500	559	646000	14400	4060	337		
Palinuro Volcanic Complex, Aeolian Island Arc, Italy																											
PVC851	5	1.06	0.148	3360	71.8	0.117	0.0214	3840	88	bdl	bdl	24.2	0.612	bdl	bdl	14100	508	30.7	1.36	787	20.4	649000	12100	2720	130	1790	103
CHALCOPYRITE (140)																											
TAG-1 (Central), TAG hydrothermal vent field, Mid-Atlantic Ridge																											
TAGM porous	8	1.86	0.328	1.98	1.38	0.0797	0.0372	0.361	0.355	88.8	6.08	1.75	0.538	bdl	bdl	0.322	0.115	0.181	0.125	347000	14300	45.7	4.74	323000	14500		
TAG6F porous	8	4.83	1.72	0.819	1.15	0.00872	0.0114	0.397	0.643	18.5	8.72	1.17	0.557	bdl	bdl	1.75	0.688	0.0501	0.0776	349000	41100	415	48.5	298000	36900		
TAG-4 (West), TAG hydrothermal vent field, Mid-Atlantic Ridge																											
TA46 porous	8	18.1	4.68	0.897	1.12	0.0209	0.0364	3.73	1.6	0.373	0.267	0.66	0.361	bdl	bdl	3.52	1.5	1.3	0.435	348000	42700	1010	409	301000	38200		
TAGJ porous	5	24.1	0.988	0.589	0.507	0.0638	0.0519	3.29	0.755	0.228	0.191	0.373	0.269	bdl	bdl	bdl	bdl	0.16	0.111	346000	8710	34.2	2.96	274000	10900		
TAG-5 (North), TAG hydrothermal vent field, Mid-Atlantic Ridge																											
TAGK massive	7	0.799	26.3	0.258	24.2	0.0127	16.8	0.426	33	1.12	14.3	0.28	47.6	bdl	bdl	bdl	bdl	0.145	46.4	347000	5490	7.62	21.6	275000	4370		
TAGL massive	8	0.628	0.127	bdl	bdl	0.0391	0.0211	0.183	0.255	0.101	0.13	0.123	0.158	bdl	bdl	bdl	bdl	0.048	0.0594	348000	9440	4.83	1.56	267000	10400		
Inactive mound, Turtle Pits hydrothermal vent field, Mid-Atlantic Ridge																											
TP2L massive	5	16.1	0.702	0.714	0.933	0.0186	0.0179	0.743	0.493	54.6	1.76	2.03	0.401	bdl	bdl	bdl	bdl	0.085	0.103	343000	10800	152	7.49	288000	11600		
TP2LTS massive	5	13.4	1.27	1.52	2.1	0.013	0.0211	1.47	2.11	65	3.35	3.03	1.08	bdl	bdl	30.2	15.9	0.401	0.472	343000	12100	146	17.1	283000	14000		
Southern Tower, Turtle Pits hydrothermal vent field, Mid-Atlantic Ridge																											
TP4BTS colloform	8	11.2	1.17	bdl	bdl	3.63	0.867	5.53	2.43	895	56.8	2.85	0.934	bdl	bdl	1.79	0.706	0.287	0.249	330000	11100	2850	274	282000	12600		
TP4B colloform	4	8.91	0.486	1.23	1.06	0.899	0.129	2.42	0.74	1130	29.4	7.75	0.438	bdl	bdl	6.19	0.949	0.389	0.159	330000	7340	801	30.7	313000	12500		
Candelaber, Logatchev-1 hydrothermal vent field, Mid-Atlantic Ridge																											

		Ag		As		Bi		Cd		Co		Mn		Ni		Pb		Sb		Cu		Zn		Fe		Hg	
Sample	**N**	**mean**	**SD**	**mean**	**SD**	**mean**	**SD**	**mean**	**SD**	**mean**	**SD**	**mean**	**SD**	**mean**	**SD**	**mean**	**SD**	**mean**	**SD**	**mean**	**SD**	**mean**	**SD**	**mean**	**SD**	**mean**	**SD**
LOG11TS massive	1	0.267	0.254	bdl	bdl	bdl	bdl	5.27	2.11	534	18.2	1.37	0.869	80.2	23.1	bdl	bdl	0.561	0.388	337000	11600	712	36.7	273000	14400		
LOG11 massive	21	8.33	0.652	3.03	2.28	1.59	0.259	2.67	1.13	976	30.5	0.716	0.378	241	14.2	2.56	0.502	0.735	0.257	337000	10500	562	31.5	280000	13900		
Irina 1, Logatchev-1 hydrothermal vent field, Mid-Atlantic Ridge																											
LOG13TS massive	2	1.35	0.369	3.13	2.52	2.43	0.569	bdl	bdl	108	5.09	1.05	0.721	49.9	23.6	1.01	0.439	bdl	bdl	348000	12600	107	10.9	278000	17700		
LOG13 massive	7	0.732	0.157	bdl	bdl	1.72	0.203	0.536	0.438	182	5.42	2.34	0.359	23.5	5.35	0.506	0.0981	bdl	bdl	348000	9340	126	10.2	283000	12200		
16°43′S hydrothermal vent field, East Pacific Rise																											
SEPR massive	5	63.9	2.39	14.2	1.83	0.0575	0.0439	1.18	0.967	56.2	2.3	1	0.499	3.46	4.67	8.04	0.897	0.455	0.226	343000	10100	217	18	282000	13600		
*Ashes hydrothermal vent field, Juan de Fuca Ridge**																											
AS1 massive	8	20.5	1.09	5.2	2.49	0.0283	0.0271	13.9	1.99	25.1	1.42	26.6	5.77	3.77	4.25	3.67	1.82	0.155	0.0868	338000	9980	3870	186	305000	15300		
Satanic Mills, Pacmanus hydrothermal vent field, Pacmanus Basin, Papua New Guinea																											
PM5E2 colloform	2	55.3	1.91	2600	86.4	19.9	0.777	0.43	0.471	0.151	0.163	0.869	0.401	bdl	bdl	127	4.67	1840	48.3	349000	8070	137	7.73	288000	9930		
PM5ETS colloform	8	75.3	3.83	4230	247	8.69	0.821	bdl	bdl	0.14	0.217	0.618	0.573	bdl	bdl	155	16.8	2320	107	349000	11200	138	24.5	273000	11300		
PM5E colloform	3	25.6	0.932	1250	38.7	34.2	1.67	0.799	0.49	bdl	bdl	0.468	0.289	bdl	bdl	69.3	2.29	1060	32.5	349000	7770	62.9	4.52	272000	10600		
PM6B2 colloform	2	101	3.51	3250	119	62.9	1.69	1.84	1.06	bdl	bdl	0.893	0.411	bdl	bdl	463	13.3	3280	94.8	342000	7660	310	15.6	266000	10400		
PM6B colloform	5	111	2.96	1310	70.9	27.5	1.46	2.12	0.808	0.11	0.151	0.471	0.278	bdl	bdl	128	5.53	1810	84.9	342000	7800	286	13.9	271000	9710		
Solwara-8, Pacmanus hydrothermal vent field, Pacmanus Basin, Papua New Guinea																											
PM2F2 massive	4	40.6	2.26	3170	170	0.0373	0.0216	3.79	1.45	bdl	bdl	1.06	0.554	bdl	bdl	248	11.9	220	12.1	353000	9690	334	17.3	269000	12200		
PM2F massive	1	13.5	0.898	4730	166	bdl	bdl	bdl	bdl	0.635	0.287	0.444	0.39	bdl	bdl	263	7.88	53.2	2.14	353000	10100	410	17.7	270000	12800		
Palinuro Volcanic Complex, Aeolian Island Arc, Italy																											
PVC932	7	8.72	0.632	130	28.4	bdl	bdl	16.8	2.67	bdl	bdl	4.07	1.85	12.5	9.64	591	76.4	176	8.63	326000	8200	1330	117	258000	11400	44.6	6.1
ISOCUBANITE (22)																											
Southern Tower, Turtle Pits hydrothermal vent field, Mid-Atlantic Ridge																											
TP4B	5	9.74	1.77	0.979	0.82	0.0405	0.0329	7.04	2.11	3490	180	19.7	1.58	13.7	14.9	6.63	2.31	0.414	0.382	257000	13000	1750	245	379000	21800		
TP4BTS	3	36.8	2.05	3.61	3.38	0.0339	0.0584	3.22	1.85	6520	173	11.5	1.21	bdl	bdl	0.238	0.315	bdl	bdl	269000	6880	2060	87	380000	11000		
Candelaber, Logatchev-1 hydrothermal vent field, Mid-Atlantic Ridge																											

		Ag		As		Bi		Cd		Co		Mn		Ni		Pb		Sb		Cu		Zn		Fe		Hg	
Sample	**N**	**mean**	**SD**	**mean**	**SD**	**mean**	**SD**	**mean**	**SD**	**mean**	**SD**	**mean**	**SD**	**mean**	**SD**	**mean**	**SD**	**mean**	**SD**	**mean**	**SD**	**mean**	**SD**	**mean**	**SD**	**mean**	**SD**
LOG11TS	2	bdl	bdl	bdl	bdl	bdl	bdl	bdl	bdl	11.5	1.53	3.68	1.19	70.2	29.3	0.691	0.354	0.632	0.402	276000	9480	71.4	12.7	375000	18900		
LOG11	8	23.7	0.821	0.259	0.53	1.01	0.0912	7.14	0.957	3840	99.1	4.5	0.394	350	12.6	0.00855	0.0211	0.0575	0.0582	296000	7290	1190	35.2	375000	15200		
BORNITE (40)																											
Candelaber, Logatchev-1 hydrothermal vent field, Mid-Atlantic Ridge																											
LOG11TS bn-cp	9	33.8	2.22	15.6	4.67	3.69	0.457	6.52	2.47	1490	436	5.1	1.02	796	115	33.7	3.12	1.2	0.486	556000	17800	2360	262	116000	5290		
Irina 1, Logatchev-1 hydrothermal vent field, Mid-Atlantic Ridge																											
LOG13TS	6	38.1	2.87	14.7	7.44	3.79	0.647	7.36	4.15	27.5	3.87	6.52	1.78	58	34.2	108	16.7	1.08	0.626	538000	7910	1710	253	116000	7770		
LOG13	2	47.4	2.11	2	1.32	0.0639	0.0326	0.207	0.275	7.87	0.557	2.04	0.356	8.19	4.77	7.38	0.597	0.121	0.126	421000	11500	175	11.1	89400	4430		
16°43'S hydrothermal vent field, East Pacific Rise																											
SEPR intergrown sp-bn-cv	5	548	27.2	28.7	3.14	0.022	0.0206	2260	229	373	43.9	31.7	3.1	1.2	2.56	162	8.63	156	10.1	293000	9060	250000	25200	148000	9590		
Solwara-8, Pacmanus hydrothermal vent field, Pacmanus Basin, Papua New Guinea																											
PM2F2 bn-cp	7	245	8.58	69.3	8.91	bdl	bdl	5.27	1.16	bdl	bdl	5.62	0.935	4.24	3.93	73.7	3.93	10.2	1.23	562000	10100	282	19.8	114000	4960		
PM2F bn-cp	2	467	16.1	821	43.6	bdl	bdl	34.6	2.88	bdl	bdl	49	2.56	bdl	bdl	830	33.9	43	1.93	562000	10300	6240	389	110000	4770		
PM2FTS intergrown bn-cp	9	395	19.5	1160	125	bdl	bdl	33.3	5.71	bdl	bdl	71.3	6.71	5.06	9.45	2070	136	88.9	13.9	562000	11600	8240	594	133000	9220		
COVELLITE-CHALCOCITE (25)																											
Candelaber, Logatchev-1 hydrothermal vent field, Mid-Atlantic Ridge																											
LOG11TS	8	8.32	1.49	7.09	2.41	1.2	0.166	174	10.9	4410	255	18.8	1.14	2680	149	513	122	9.31	2.48	697000	11000	17100	877	26200	1410		
Irina 1, Logatchev-1 hydrothermal vent field, Mid-Atlantic Ridge																											
LOG13TS	8	70.1	4.19	2.52	2.38	22.2	1.84	24.2	4.03	105	12.2	11.5	1.72	172	27.7	40.6	8.53	1.18	0.53	659000	12100	5780	578	24500	2340		
LOG13 cv-dg	4	74	8.8	11.1	1.93	15.9	0.825	2.49	0.846	105	4.97	50.5	2.83	154	12.7	34.7	1.6	3.38	0.304	602000	14600	1130	43.9	169000	7660		
16°43'S hydrothermal vent field, East Pacific Rise																											
SEPR	1	818	42.4	38.2	4.25	bdl	bdl	477	25.6	49.9	3.72	6.67	0.558	bdl	bdl	248	25.5	190	15.3	564000	15700	43300	2680	81700	7320		
Solwara-8, Pacmanus hydrothermal vent field, Pacmanus Basin, Papua New Guinea																											
PM2F2 cc-cv	8	664	27.5	621	74.1	bdl	bdl	18.6	5.29	bdl	bdl	415	16.7	bdl	bdl	219	26.7	75.1	3.58	721000	11900	6640	519	29900	1600		
PYRITE (142)																											
TAG-1 (Central), TAG hydrothermal vent field, Mid-Atlantic Ridge																											
TAGM massive	3	0.272	0.0771	75.4	7.47	bdl	bdl	bdl	bdl	50.2	6.64	5.63	0.553	bdl	bdl	7.82	1.06	1.38	0.168	54.4	5.28	5.54	1.55	463000	18500		
TAG6F massive	7	0.251	0.089	30.6	7.89	0.0254	0.0173	0.202	0.225	182	55	0.707	0.291	bdl	bdl	10.6	4.17	0.321	0.0912	180	43.3	2.9	1.85	464000	92000		
TAG6F colloform interior	4	0.316	0.144	45.5	11.7	0.151	0.0434	0.0829	0.0838	636	64.8	0.933	0.478	bdl	bdl	1.74	0.22	0.545	0.246	1930	358	169	146	464000	35200		
TAG6F	2	0.194	0.0687	67.2	11.3	0.0485	0.0242	bdl	bdl	813	87	2.09	0.494	bdl	bdl	1.15	0.154	0.748	0.15	555	150	39.2	12.3	462000	35300		

Sample	N	Ag mean	Ag SD	As mean	As SD	Bi mean	Bi SD	Cd mean	Cd SD	Co mean	Co SD	Mn mean	Mn SD	Ni mean	Ni SD	Pb mean	Pb SD	Sb mean	Sb SD	Cu mean	Cu SD	Zn mean	Zn SD	Fe mean	Fe SD	Hg mean	Hg SD
colloform exterior TAG27 porous	8	0.355	0.114	47.4	8.77	0.185	0.0908	bdl	bdl	404	101	1.58	0.635	bdl	bdl	20.5	6.76	0.722	0.197	484	150	7.53	2.98	461000	62200		
TAG-4 (West), TAG hydrothermal vent field, Mid-Atlantic Ridge																											
TAGH massive	6	0.721	0.108	32.1	2.77	bdl	bdl	0.178	0.131	8.61	1.46	7.6	0.819	1.96	1.12	55	4.48	0.831	0.0891	27.3	3.98	12.9	2.3	464000	20000		
TAGI colloform	2	bdl	bdl	60.8	7.26	0.0256	0.0144	0.112	0.139	0.0549	0.0852	11.6	0.478	bdl	bdl	243	29.1	2.26	0.169	1.67	1.07	24.1	1.94	459000	20000		
TAGI colloform	3	bdl	bdl	178	8.09	0.022	0.0141	bdl	bdl	0.177	0.106	1.87	0.176	1.77	1.14	225	12.8	10.7	0.723	1.97	0.676	4.69	1	444000	22700		
TAG47 massive	9	2.33	0.428	47.9	8.16	bdl	bdl	2.1	0.739	10.5	2.41	17.9	1.23	bdl	bdl	92.4	14.2	2.07	0.266	75.3	9.58	836	186	462000	30900		
TAG46 massive	8	7.32	2.41	325	106	bdl	bdl	0.119	0.172	13.2	5.91	72	19	2.04	1.54	111	21.5	3.38	0.591	169	27.2	45.3	8.04	463000	54200		
TAG48 massive	10	6.35	2.1	56.1	6.03	bdl	bdl	0.81	0.589	19.4	4.6	18.8	11.8	5.75	4.39	101	13.6	3.23	0.68	61.1	11.2	572	326	458000	40000		
TAG48 colloform interior	1	0.505	0.157	8.1	1.95	bdl	bdl	bdl	bdl	3.41	0.252	55.7	1.84	17.5	13.4	59.6	3.59	0.822	0.436	10.2	2.55	95.6	7.47	458000	54400		
TAG48 colloform exterior	2	4.96	0.731	8.62	2.09	0.0352	0.0212	0.524	0.407	3.02	0.33	41.4	1.91	bdl	bdl	61.5	3.45	1.13	0.256	55.8	7.37	626	125	444000	46600		
TAGJ massive	6	15.7	1.36	104	7.27	0.133	0.0306	0.167	0.153	73.7	7.6	5.87	0.598	7.45	2.14	175	16.1	8.26	0.9	579	44.3	43	6.72	462000	27100		
TAG-5 (North), TAG hydrothermal vent field, Mid-Atlantic Ridge																											
TAGK massive	3	0.252	14.9	33.9	7.48	0.131	14.5	0.109	32	237	7.68	0.707	22.3	bdl	bdl	5.6	8.37	0.387	23	261	7.94	7.3	32.1	464000	5440		
TAGL porous	2	bdl	bdl	1.33	0.421	bdl	bdl	0.0807	0.115	3.41	0.764	0.236	0.108	1	1.05	0.0123	0.0139	bdl	bdl	11.7	2.72	0.728	0.512	465000	18100		
Inactive mound, Turtle Pits hydrothermal vent field, Mid-Atlantic Ridge																											
TP2L massive	8	0.106	0.1	78.2	8	0.0116	0.0181	0.129	0.245	674	125	0.92	0.513	0.302	0.87	1.66	0.907	0.0163	0.0258	46.2	14.6	1.71	1.91	460000	37100		
TP2LTS massive	6	3.23	0.476	1360	139	0.01	0.0205	0.66	0.662	260	61.5	14.6	2.14	2.66	5.1	69.5	12.8	6.03	0.652	433	66.7	503	143	460000	34800		
TP2LTS colloform	5	12.2	0.986	29.7	3.58	0.0116	0.022	0.512	0.611	331	48.3	522	26.1	3.25	4.58	92.5	11.4	1.13	0.302	2770	140	140	11.2	444000	28600		
TP2L colloform	2	3.93	0.332	6.36	0.856	bdl	bdl	0.557	0.252	23.5	2.08	65	5.26	2.25	2.22	735	37.7	0.629	0.105	3990	228	459	444000	25300	3.93		
TP2L colloform	4	12	0.734	20.5	1.66	bdl	bdl	0.366	0.263	174	9.86	167	9.17	5.33	2.8	638	37.1	1.42	0.165	4940	303	427	444000	22900	12		

Sample	N	Ag		As		Bi		Cd		Co		Mn		Ni		Pb		Sb		Cu		Zn		Fe		Hg	
		mean	SD	mean	SD	mean	SD	mean	SD	mean	SD	mean	SD	mean	SD	mean	SD	mean	SD	mean	SD	mean	SD	mean	SD	mean	SD
Southern Tower, Turtle Pits hydrothermal vent field, Mid-Atlantic Ridge																											
TP4B porous	17	1.3	0.231	280	33.6	0.0182	0.0145	0.327	0.346	257	83.3	2.1	0.76	0.638	1.03	158	14.2	0.94	0.23	347	305	18.3	11	463000	26200		
16°43'S hydrothermal vent field, East Pacific Rise																											
SEPR massive	4	8.99	0.606	59	4.05	0.0162	0.0163	0.42	0.34	48.5	2.32	82.8	3.56	2.01	1.97	259	11.1	2.76	0.329	10.4	1.69	427	26.4	461000	27600		
*Ashes hydrothermal vent field, Juan de Fuca Ridge**																											
AS1 massive	6	bdl	bdl	177	18.9	0.0159	0.0234	0.394	0.373	245	29.6	0.756	0.359	2.72	3.81	3.27	1.01	0.0933	0.0741	5.93	3	38.8	22.1	461000	34400		
AS1 colloform	5	8.59	0.655	273	13	bdl	bdl	0.594	0.358	8.39	0.544	141	5.57	9.87	3.35	154	6	4.82	0.387	3970	159	202	11.1	456000	22200		
Roman Ruins, Pacmanus hydrothermal vent field, Pacmanus Basin, Papua New Guinea																											
PM2D2 massive	3	0.601	0.104	2700	83.5	bdl	bdl	0.212	0.199	0.0606	0.0593	7.45	0.568	0.656	1.07	266	8.06	103	5.36	1.76	0.421	8.55	1.4	463000	22200		
PM2D massive	5	0.0426	0.0493	5080	153	bdl	bdl	0.124	0.105	0.0567	0.0655	12	0.435	bdl	bdl	88.8	2.8	29.2	0.934	0.375	0.341	7.27	1.35	463000	17200		
Satanic Mills, Pacmanus hydrothermal vent field, Pacmanus Basin, Papua New Guinea																											
PM6B2 colloform	2	440	14.8	12200	361	bdl	bdl	12.9	1.9	0.0412	0.0685	258	6.99	bdl	bdl	6170	268	55.1	3.22	4430	224	24200	2070	428000	23400		
PM6B colloform	2	288	10.2	13300	391	0.192	0.0468	12.2	2.42	1.67	0.328	1040	45.2	46.2	3.82	12700	860	877	33	5000	1900	54300	24600	428000	17100		
Palinuro Volcanic Complex, Aeolian Island Arc, Italy																											
PVC851	8	bdl	bdl	8240	243	bdl	bdl	bdl	bdl	bdl	bdl	3520	111	bdl	bdl	302	33	25.7	2.27	20.1	1.68	292	28.1	470000	20000	bdl	bdl
PVC932	8	bdl	bdl	4680	157	bdl	bdl	bdl	bdl	bdl	bdl	5320	161	bdl	bdl	0.713	0.268	1.71	0.18	bdl	bdl	33.4	2.37	442000	21100	bdl	bdl
MARCASITE (78)																											
TAG-1 (Central), TAG hydrothermal vent field, Mid-Atlantic Ridge																											
TAGM massive	3	0.338	0.103	81.6	8.46	bdl	bdl	0.274	0.275	43.8	5.78	64.2	9.85	bdl	bdl	19	2.59	0.558	0.14	57.2	6.01	6.3	1.26	463000	25500		
TAG-4 (West), TAG hydrothermal vent field, Mid-Atlantic Ridge																											
TAGH massive	4	3.02	0.26	31.6	2.78	bdl	bdl	0.414	0.218	1.99	0.327	6.46	0.565	1.27	1.43	94.1	12.3	0.52	0.105	36.5	3.47	31.1	3.53	464000	20200		
TAGI colloform	3	0.134	0.0632	13.8	1.58	bdl	bdl	0.146	0.0973	0.368	0.142	4.71	0.407	5.15	2.18	802	50.1	3.12	0.242	1.27	0.966	9.21	1.72	459000	19100		
TAG47 massive	8	0.399	0.131	8.38	1.54	bdl	bdl	0.642	0.371	1.56	0.626	5.87	0.594	1.98	2.49	9.24	1.15	0.735	0.142	18.1	2.95	214	47.4	461000	20700		
TAG46 massive	8	5.76	0.826	73.7	13.3	bdl	bdl	0.623	0.422	10.3	2.29	4.73	0.904	1.39	2.25	54.2	15.5	1.23	0.221	63.6	11.5	20	6.56	461000	53100		
TAG48 massive	8	1.77	0.368	7.96	2.33	bdl	bdl	bdl	bdl	0.719	0.231	13.7	2.07	2.67	2.82	12.3	1.7	1.03	0.207	39.5	7.32	152	27.1	459000	38200		
TAG48 colloform	3	3.28	3.76	9.32	1.95	bdl	bdl	0.432	0.406	8.71	0.602	42.6	4.95	4.1	3.62	167	15.5	1.53	0.276	62.2	10.3	1010	245	455000	31400		
TAGJ massive	3	8.78	0.619	30.1	2.81	bdl	bdl	0.164	0.137	0.564	0.167	5.93	0.312	2.85	2.22	53.2	5.35	2.83	0.247	62.5	5.83	17.7	1.87	463000	17300		
Inactive mound, Turtle Pits hydrothermal vent field, Mid-Atlantic Ridge																											
TP2LTS colloform	8	1.03	0.281	4.12	2.22	bdl	bdl	bdl	bdl	43.9	6.9	41.3	6.06	bdl	bdl	184	16.9	0.68	0.235	1070	110	64.2	9.43	460000	28200		

Sample	N	Ag mean	Ag SD	As mean	As SD	Bi mean	Bi SD	Cd mean	Cd SD	Co mean	Co SD	Mn mean	Mn SD	Ni mean	Ni SD	Pb mean	Pb SD	Sb mean	Sb SD	Cu mean	Cu SD	Zn mean	Zn SD	Fe mean	Fe SD	Hg mean	Hg SD
Southern Tower, Turtle Pits hydrothermal vent field, Mid-Atlantic Ridge																											
TP4B porous	7	4.83	0.49	478	39.3	bdl	bdl	bdl	bdl	146	15.3	3.54	0.64	0.458	0.816	328	21.9	1.1	0.262	410	51.2	47.8	12.1	461000	30300		
TP4BTS colloform	8	3.39	0.602	193	44.3	bdl	bdl	0.433	0.5	282	37.9	1.95	0.644	bdl	bdl	64.7	9.1	0.908	0.352	2330	295	39.3	11.3	463000	19700		
*Ashes hydrothermal vent field, Juan de Fuca Ridge**																											
AS1 massive	6	4.25	0.822	648	42.3	bdl	bdl	0.184	0.159	64.4	8.1	1100	54.9	13.4	11.6	51.2	3.65	1.13	0.444	1240	111	335	37.8	464000	30200		
Roman Ruins, Pacmanus hydrothermal vent field, Pacmanus Basin, Papua New Guinea																											
PM2D2 massive	1	0.283	0.0659	594	19.1	bdl	bdl	0.253	0.202	bdl	bdl	9.64	0.365	bdl	bdl	859	23.4	583	14.8	1.36	0.565	11.7	1.18	462000	20300		
Satanic Mills, Pacmanus hydrothermal vent field, Pacmanus Basin, Papua New Guinea																											
PM5E2 massive	8	0.495	0.201	247	18.5	bdl	bdl	bdl	bdl	bdl	bdl	312	13.4	2.11	7.23	9.32	1.72	0.138	0.158	6.73	2.67	20.8	8.29	464000	29400		
GALENA (23)																											
Roman Ruins, Pacmanus hydrothermal vent field, Pacmanus Basin, Papua New Guinea																											
PM2D2	1	600	31.8	bdl	bdl	bdl	bdl	5.71	0.825	0.171	0.134	0.316	0.22	4.81	3.46	843000	13900	3240	82.5	3.77	0.898	3.4	3.51	bdl	bdl		
PM2D	3	8580	247	191	54.5	15.1	0.367	0.182	0.178	bdl	bdl	0.0489	0.0611	0.767	0.933	843000	7950	26500	610	49.9	1.32	11.9	1.21	8.88	8.85		
PM2DTS	8	4580	151	137	11.4	bdl	bdl	1.25	0.426	bdl	bdl	0.332	0.143	bdl	bdl	843000	21600	32300	784	156	5.31	759	334	33.6	18.8		
Satanic Mills, Pacmanus hydrothermal vent field, Pacmanus Basin, Papua New Guinea																											
PM6BTS	5	471	28.7	5570	253	9.08	0.525	77.2	11.8	0.27	0.239	1.84	0.558	bdl	bdl	859000	10800	3150	194	112	19.2	6910	1020	211	125		
Palinuro Volcanic Complex, Aeolian Island Arc, Italy																											
PVC851	2	2.31	0.197	1560	25.8	8.03	0.13	52.1	2.93	bdl	bdl	0.502	0.192	bdl	bdl	847000	7250	8550	164	63.4	1.77	2490	484	bdl	bdl	211	13.1
PVC932	16	39.8	1.43	4970	219	7.8	0.196	41.8	1.58	bdl	bdl	0.416	0.0361	bdl	bdl	864000	6990	60.3	10.5	49.7	1.72	78.1	37.4	bdl	bdl	48.8	3.52
TENNANTITE-TETRAHEDRITE (23)																											
Satanic Mills, Pacmanus hydrothermal vent field, Pacmanus Basin, Papua New Guinea																											
PM5E2	5	932	28.8	261000	9370	2.79	0.233	313	14.5	0.513	0.145	6.19	0.562	7.28	10.8	1240	50	18300	925	407000	6420	37000	1250	43600	1810		
PM5E	6	695	17.8	236000	9540	8.06	0.572	286	15	0.751	0.219	5.26	0.36	1.08	1.61	2980	184	18200	1060	407000	5610	32500	1180	43400	3160		
PM6B2	2	3670	209	211000	7800	23.4	1.08	1810	232	0.189	0.145	6.67	1.35	5.93	4.11	12000	1060	32700	1240	319000	6050	141000	14500	15600	1010		
Solwara-8, Pacmanus hydrothermal vent field, Pacmanus Basin, Papua New Guinea																											
PM2F2	8	85.9	2.84	236000	10900	0.069	0.0386	433	21	0.16	0.21	35.4	5.95	1.28	2.71	1970	96.7	2070	193	402000	7320	49100	1830	36200	1550		
PM2F	2	447	10.4	246000	9140	bdl	bdl	455	17.7	bdl	bdl	3.46	0.321	bdl	bdl	655	24.2	5440	203	402000	7390	59400	1690	35900	1260		
Palinuro Volcanic Complex, Aeolian Island Arc, Italy																											
PVC9832	8	4740	121	141000	3970	4.21	0.859	981	40.3	bdl	bdl	6.71	0.972	bdl	bdl	1290	222	193000	5150	394000	2970	63800	1630	29400	1470	3210	177
PYRRHOTITE (10)																											
Southern Tower, Turtle Pits hydrothermal vent field, Mid-Atlantic Ridge																											
TP4BTS	3	7.12	2.02	n/a	n/a	0.817	0.395	23.1	9	2370	73.8	8.33	2.56	47.7	31.7	940	149	13.8	3.14	n/a	n/a	n/a	n/a	598000	24200		

Table S7 Trace element distribution in various sulfides from a range of samples (where no LA-ICP-MS data available) from EMPA in ppm and 2 sigma standard deviation. N;number of analysis bdl; below the minimum detection limit

		As		Sb		Cu		Zn		Fe		Mn		S		Hg		Co		Pb	
Sample	**N**	**mean**	**SD**	**mean**	**SD**	**mean**	**SD**	**mean**	**SD**	**Mean**	**SD**	**Mean**	**SD**	**Mean**	**SD**	**Mean**	**SD**	**Mean**	**SD**	**Mean**	**SD**
PYRRHOTITE (40)																					
Southern Tower, Turtle Pits hydrothermal vent field, Mid-Atlantic Ridge																					
TP4BTS	26	Bdl	bdl			3800	100	600	100									3800	100		
TP4B	14	Bdl	bdl			3200	300	1100	100									n/a	n/a		
COLLOFORM PYRITE (25)																					
Satanic Mills, Pacmanus hydrothermal vent field, Pacmanus Basin, Papua New Guinea																					
PM6B	10	9417.92	321.38	88.33	72.51	4799.96	259.84	12166.51	204.71	429342.57	19396.39	640.07	75.73	516056.07	16401.01						
PM5E	9	8625.29	323.31	Bdl	bdl	6865.43	41840.41	18230.92	345.63	416249.80	18850.21	861.31	81.78	516164.68	16415.76						
Palinuro Volcanic Complex, Aeolian Island Arc, Italy																					
PVC932	6																				
colloform		4400	200	Bdl	Bdl	Bdl	Bdl									Bdl	Bdl			4600	400
COLLOFORM CHALCOPYRITE (19)																					
Satanic Mills, Pacmanus hydrothermal vent field, Pacmanus Basin, Papua New Guinea																					
PM6B	7	823.34	201.95	860.06	94.79	345870.44	11640.6	1984.99	105.86	304808.39	12185.79	Bdl	Bdl	346378.39	9809.51						
PM5E	7	628.49	130.93	321.46	74.84	347971.49	13906.11	6018.01	138.5	298464.53	13497.67	Bdl	bdl	346580.8	11051.08						
PM5E	2	541.45	111.51	393.15	74.36	351138.8	14031.45	1919.65	79.89	299449.8	13540.36	Bdl	Bdl	345138.35	11005.83						
PM5E	3	2607.2	152.81	1716.27	89.33	320451.7	12890.05	17721.7	321.77	278106.83	12597.37	Bdl	bdl	329060	10498.83						
GALENA (80)																					
Satanic Mills, Pacmanus hydrothermal vent field, Pacmanus Basin, Papua New Guinea																					
PM2D	19	Bdl	Bdl	16100	300	100	100									100	100			836500	7900
PM5E	2	35200	900	Bdl	Bdl	700	100									100	100			845100	7900
PM6BTS	12	7500	200	3000	100	Bdl	Bdl									Bdl	bdl			859500	8000
PVC932	19	4200	100	200	100	Bdl	Bdl									100	100			864200	0.81
PVC851	28	1800	100	10800	200	bdl	bdl									300	100			846600	0.79
SPHALERITE (7)																					
Palinuro Volcanic Complex, Aeolian Island Arc, Italy																					
PVC851	7									2800	100										
colloform		2600	100	Bdl	Bdl	900	100									9400	200			15700	600
TENNANTITE-TETRAHEDRITE (6)																					
Palinuro Volcanic Complex, Aeolian Island Arc, Italy																					
PVC932	6	100200	2600	156700	2300	393600	3300									1700	300			3900	900

Table S8 Trace element contents (ppm) of common sulfide minerals from SMS deposits derived from electron microprobe analysis (EPMA), laser ablation inductively coupled mass spectrometry (LA-ICPMS) and bulk analysis of mineral concentrates. *Abbreviations used:* MAR, Mid Atlantic Ridge; EPR, East Pacific Rise; JDFR, Juan de Fuca Ridge; PNG, Papua New Guinea.

No.	Ag	As	Cd	Co	Cu	Pb	Sb	Zn	Other	Location (setting)	Authors
						Pyrrhotite ($Fe_{(1-x)}S$)					
27	200		200-300	600-4000	200			200-1900	100-1100 Ni	Rainbow vent field, MAR	Marques et al. (2006)
	400 -700		0-400		100-600			0-700		Southern JDFR	Paradis et al. (1988)
14	<400	<300 – 750			650			<600 - 800	<300 Se	Endeavour Segment, JDFR	Tivey et al. (1999)
						Marcasite (FeS_2)					
2		783-928	137-154	60-200			40-74			Axial Seamount, JDFR	Hannington et al. (1991)
			0	0	100			800	100 Ni	Alice Spring Field, Mariana Trough	Iwaida and Ueno (2005)
3-26	10.6	30.2	87.8	60.5	67.7	1.96	201.3	10.6	Avg 4.35 Mn Avg 16.9 Ni Avg 0.24 Bi	TAG hydrothermal field, MAR	Grant et al. (2018)
						Pyrite/Marcasite (FeS_2)					
22	0.31-412	41-2200	0-79	2.88-666.26	76-38000	7.4-6400	0.48-255.21	4-48090	0.5-157.7 Ni 0.003-668.15 Tl	Menez Gwen Field, MAR	Lein et al. (2010)
161		600							Max 600 Hg, Avg <200	Hook Ridge, Antarctica	Petersen et al. (2004)
				<200	<200		<200	<200			
85	<400	750-1676		<400	<700 – 2570	<1200	<100	<600 - 750	<400 – 3900 Mn	Endeavour Segment, JDFR	Tivey et al. (1999)
20		bdl-7200			bdl-2000			1550-8477	Avg 6333 Mn	Mothra hydrothermal field, JDFR	Kristall et al. (2006)
						Pyrite (FeS_2)					
1	62	115	<10	51			5		124 Mo	TAG hydrothermal field, MAR	Hannington et al. (1991)
167	<400	<400		<400 – 1460	<600 - 2686	<1200 – 7075		<600 - 8783	<300 – 430 Se	TAG hydrothermal field, MAR	Tivey et al. (1995)
70-252	3.42	46	1.29	447.7	132	36.9	2.73	51	Avg 13.1 Mn Avg 22 Ni Avg 0.45 Bi	TAG hydrothermal field, MAR	Grant et al. (2018)
4	14-95	436-1740	<10-10	2-85			4-19		47-62 Mo <2 to 98 Se	Snakepit vent field, MAR	Hannington et al. (1991)
49	100		100	1200-	1000			400-3000	Avg 300 Ni	Rainbow vent field, MAR	Marques et al. (2006)

No.	Ag	As	Cd	Co	Cu	Pb	Sb	Zn	Other	Location (setting)	Authors
				1800							
40		224					4.94		Avg 25.2 Se, 0.25 Au, 1.2 Te	Turtle Pits, MAR	
											Wohlgemuth-Ueberwasser et al.
38		257			500	bdl	bdl	937.5		Turtle Pits, MAR	(2015)
23		326					11.2		Avg 15.5 Se, 4.18 Au, 0.58 Te	Logatchev, MAR	
											Wohlgemuth-Ueberwasser et al.
6		bdl			300	bdl	bdl	bdl		Logatchev, MAR	(2015)
3	18	664.3	26.6	36			10.3		20-200 Se	Southern Explorer Ridge	Hannington et al. (1991)
16	<200	600	<200	200	3600	200	<200	1300	Avg 400 Ni Avg 200 Se	Kairei vent field, Indian Ridge	Wang et al. (2014)
19	143	224	8.71	110	500	444	3.91	300	Avg 538 Mn Avg 36.4 Se	Wocan hydrothermal field, Carlsberg Ridge, Indian Ocean	Wang et al. (2017)
26	85	312	613	2554	217	69	45	1784	Avg 9 Ni Avg 84 Au	Longqi, Southwest Indian Ridge	(Zhang et al., 2018)
22	98	407	134	919	1020	1103	23	11855	Avg 16 Ni Avg 229 Au	Duanqiao, Southwest Indian Ridge	(Zhang et al., 2018)
6		800-2600		1000-12100	800-2400					Green Seamount, EPR	Alt et al. (1987)
339	<200	2950	<200		2300	3350	450	550	Max 6900 Hg, Avg <300	Palinuro Volcanic Complex, Aeolian Arc, Italy	Petersen et al. (2014)
3			0-100	400-600	500-11700			0-3500	0 Ni	Alice Spring Field, Mariana Trough	Iwaida and Ueno (2005)
3		0-500							0-200 Au	North Knoll, Iheya Ridge, Okinawa Trough	Ueno et al. (2003)
58		2635					188		Avg 7.39 Se, 7.71 Au, 1.1 Te	Roman Ruins, Pacmanus Basin, PNG	
44		3636			2200	3236	144	4981		Roman Ruins, Pacmanus Basin, PNG	Wohlgemuth-Ueberwasser et al. (2015)
5		5390					29.4		Avg 5.97 Se, 8.16 Au, bdl Te	Satanic Mills, Pacmanus Basin, PNG	
2		bdl			8200	4100	bdl	2900	Sphalerite ((ZnFe)S)	Satanic Mills, Pacmanus Basin, PNG	
34	0-1700	0-10100	0-9000		0-7900	0	0-1300		0-900 In, Ni 3600-18000 Fe	Menez Gwen Field, MAR	Lein et al. (2010)
3	49-206	66-93	599-1646	55-101			25-56		<0.1-5.7 Au <1-30 Mo, <2-23 Se	TAG hydrothermal field, MAR	Hannington et al. (1991)
88	<400 – 917		1400-3076		1804-9988	<1000 – 1600	<400 - 900		6094-34006 Fe <300 Mn	TAG hydrothermal field, MAR	Tivey et al. (1995)

No.	Ag	As	Cd	Co	Cu	Pb	Sb	Zn	Other	Location (setting)	Authors
4-19	58.5	63	1202	19.6	1364	125	41.3		Avg 24191 Fe Avg 17.4 Mn Avg 10.2 Ni Avg 0.04 Bi	TAG hydrothermal field, MAR	Grant et al. (2018)
2	430-1147	769-881	515-829	7-18			138-163		10.7-18.3 Au 25-29 Mo, <2 Se	Snakepit vent field, MAR	Hannington et al. (1991)
5	1000		600	100	2200				Avg 14000 Fe	Rainbow vent field, MAR	Marques et al. (2006)
20		147					47.9		0.36 Au, 28.2 Se, 0.62 Te	Turtle Pits, MAR	Wohlgemuth-Ueberwasser et al. (2015)
6		100			1450	bdl	bdl		142000 Fe	Turtle Pits, MAR	
10		214					223		3.73 Au, 1.68 Se, 0.73 Te	Logatchev, MAR	Wohlgemuth-Ueberwasser et al. (2015)
8		300			11400	bdl	300		114500 Fe	Logatchev, MAR	
12	<200	400	1000	400	9000	1500	<200		Avg 62900 Fe <200 Ni, Se	Kairei vent field, Indian Ridge	Wang et al. (2014)
17	96.9	726	3085	0.06	12530	1718	86		Avg 16066 Fe Avg 131 Ga, 200 Ge	Wocan hydrothermal field, Carlsberg Ridge, Indian Ocean	Wang et al. (2017)
18	133	149	1950	186	3260	178	74		Avg 54 Ni Avg 133 Au	Longqi, Southwest Indian Ridge	(Zhang et al., 2018)
19	385	61	525	161	1010	225	64		Avg 19 Ni Avg 35 Au	Duanqiao, Southwest Indian Ridge	(Zhang et al., 2018)
65	4200	6600	2100		13400	4600	<200		Avg 1200 Fe, 600 Ga Avg 2700 Hg, 300 Tl	Hook Ridge, Antarctica	Petersen et al. (2004)
6			5700-11900		700-5600				2900-77100 Fe	Green Seamount, EPR	Alt et al. (1987)
5	210-400	108-364	1820-3150				355-1580		1.1-3.1 Au	Axial Seamount, JDFR	Hannington et al. (1991)
					0-10000				<10000-80000 Fe		Hannington and Scott (1988)
34	0-2100		0-5600		0-5100				3500-117000 Fe	Southern JDFR	Paradis et al. (1988)
30			300-3500						700-187000 Fe	North Cleft, JDFR	Koski et al. (1994)
			0-4400		0-8100						
3									9000-150000 Fe, 0-200 Mn	South Cleft, JDFR	Normark et al. (1983)
311	<200	4600	3800		2600	12900	2200		Avg 8000 Fe, 7400 Hg	Palinuro Volcanic Complex, Aeolian Arc, Italy	Petersen et al. (2014)
6		0-1000	5200-		800-				500-4300 Fe	Hakurei Deposit, Bayonnaise Knoll,	Watanabe and Hayashi (2014)

No.	Ag	As	Cd	Co	Cu	Pb	Sb	Zn	Other	Location (setting)	Authors
			6300		6500					Uzu-Bonin Arc	
4			500-5300		1800-12300				189100-236100 Fe 6300-120400 Mn	Escanaba Trough, Gorda Ridge	Zierenberg and Shanks (1983)
15					3000-7000				<1000-27000 Fe <1000-4000 Mn	Central Okinawa Trough	Halbach et al. (1993)
8			1200-3300	0-300	0-500				10900-26200 Fe 1600-4700 Mn, 0-600 Ni	North Knoll, Iheya Ridge, Okinawa Trough	Ueno et al. (2003)
82			400-900		1100-13700				2100-106800 Fe 2600-15600 Mn	Yonaguni Knoll, Okinawa Trough	Suzuki et al. (2008)
7			200-5000		0-8900				2900-58200 Fe 100-1200 Mn	Alice Spring Field, Mariana Trough	Iwaida and Ueno (2005)
			300-1700						150600-241200 Fe 900-7000 Mn	Guaymas Basin, Gulf of California	Koski et al. (1985)
7	700	11000			38000	15000	<500		20000 Fe	Pacmanus Chimney, PNG	Binns and Scott (1993)
52		1664					1576		43.3 Au, 3.57 Se, 0.02 Te	Roman Ruins, Pacmanus, PNG	
24		1216.6			3433.3	1760	1700		35766.6 Fe	Roman Ruins, Pacmanus, PNG	Wohlgemuth-Ueberwasser et al. (2015)
6		17269					167		2.45 Au, 9.42 Se, bdl Te	Satanic Mills, Pacmanus, PNG	
3		1600			5600	23500	100		7000 Fe	Satanic Mills, Pacmanus, PNG	
								Sphalerite – Wurtzite ((ZnFe)S)			
30					bdl-38500				45300-119200 Fe 500-3300 Mn	Mothra hydrothermal field, JDFR	Kristall et al. (2006)
44	<400	<300 – 400	1580	<200	<700-9100	<1000 – 2550	<400		<300 – 6542 Mn <500 – 246793 Fe	Endeavour Segment, JDFR	Tivey et al. (1999)
								Wurtzite ((ZnFe)S)			
7	0-900		400-7100		1500-8100				65200-165500 Fe	Southern JDFR	Paradis et al. (1988)
33			1150-7000						32100-175000 Fe	North Cleft, JDFR	Koski et al. (1994)
2			0-2900		0				36000-128000 Fe	South Cleft, JDFR	Normark et al. (1983)
4			1700-4200	0-600	0-2200				21600-60700 Fe 4600-10000 Mn	North Knoll, Iheya Ridge, Okinawa Trough	Ueno et al. (2003)

No.	Ag	As	Cd	Co	Cu	Pb	Sb	Zn	Other	Location (setting)	Authors
									0-700 Ni		
					1900						
19			1500						28800 Fe	Yonaguni Knoll, Okinawa Trough	Suzuki et al. (2008)
									3200 Mn		
									Chalcopyrite ($CuFeS_2$)		
	58-378		2-258			0-379	0-110.83	180-26100	0-129 Mn	Menez Gwen Field, MAR	Lein et al. (2010)
									0.32-953 Mo		
									101-770 Se		
									0-116.2 V		
	13-48	6-65	<10	113-1053			0.4-5		0.2-0.9 Au	TAG hydrothermal field, MAR	Hannington et al. (1991)
									98-498 Co		
									205-640 Se		
90	<400			<400		<1000		1223-9820	<300 – 1060 Se	TAG hydrothermal field, MAR	Tivey et al. (1995)
10-50									Avg 0.46 Bi	TAG hydrothermal field, MAR	Grant et al. (2018)
	8.98	7.21	3.85	39.8	346300	5.74	0.67	192.1	Avg 1.61 Mn		
									Avg 24.5 Ni		
35	100-700		200-600	200-2000				1300-12100	100-400 Ni	Rainbow vent field, MAR	Marques et al. (2006)
								416			Mozgova et al. (2005)
10	150			3150					1150 Au		
									1400 Ni		
15		37.9					0.46		0.06 Au, 204 Se, 4.73 Te	Turtle Pits, MAR	Wohlgemuth-Ueberwasser et al. (2015)
24		bdl				bdl	bdl	1140		Turtle Pits, MAR	
29		92.4					22		3.12 Au, 119 Se, 39.2 Te	Logatchev, MAR	Wohlgemuth-Ueberwasser et al. (2015)
18		300				bdl	100	1550		Logatchev, MAR	
	<5	49-100	<10	19-383			0.6-0.7		<0.1 Au	Southern Explorer Ridge	Hannington et al. (1991)
									77-443 Mo		
									190-310 Se		
33	<200	<200	<200	<200		<200	<200	100	<200 Ni	Kairei vent field, Indian Ridge	Wang et al. (2014)
									300 Se		
22	65.3	225	46.9	0.1		120	22	1040	Avg 50 Se	Wocan hydrothermal field, Carlsberg Ridge, Indian Ocean	Wang et al. (2017)
									Avg 80.8 Ge		
11	330	192	141	748		41	43	6253	Avg 23 Ni	Longqi, Southwest Indian Ridge	(Zhang et al., 2018)
									Avg 149 Au		
16	289	162	77	616		67	89	1247	Avg 23 Se	Duanqiao, Southwest Indian Ridge	(Zhang et al., 2018)
									Avg 18 Ni		

No.	Ag	As	Cd	Co	Cu	Pb	Sb	Zn	Other	Location (setting)	Authors
									Avg 135 Au		
	100-1500		100-700					1700-10400		Southern Juan de Fuca Ridge	Paradis et al. (1988)
105	<200	<1000	<200			<2000	900	300	100 Hg	Palinuro Volcanic Complex, Aeolian Arc, Italy	Petersen et al. (2014)
4			125					3925	100 Mn	Alice Spring Field, Mariana Trough	Iwaida and Ueno (2005)
4			0					14850	400 Mn	North Knoll, Iheya Ridge, Okinawa Trough	Ueno et al. (2003)
5	<500	800				<1400	<400	<500		Pacmanus Chimney, PNG	Binns and Scott (1993)
75		470					84.5		4.84 Au, 23.5 Se, 0.32 Te	Roman Ruins, Pacmanus, PNG	Wohlgemuth-Ueberwasser et al. (2015)
43		bdl				160	100	2350		Roman Ruins, Pacmanus, PNG	
25		15237					875		4.99 Au, 1.39 Se, 1.66 Te	Satanic Mills, Pacmanus, PNG	
15		bdl				200	300	5850		Satanic Mills, Pacmanus, PNG	
									Chalcopyrite ($CuFeS_2$) – Isocubanite ($CuFe_2S_3$)		
64	<400	<400 – 600		<400		<1000	<100	1600 – 12150	<400 Mn	Endeavour Segment, JDFR	Tivey et al. (1999)
									Isocubanite ($CuFe_2S_3$)		
10		22.4					7.63		8.15 Au, 40.9 Se, 7.9 Te	Logatchev, MAR	Wohlgemuth-Ueberwasser et al. (2015)
8		bdl				bdl	bdl	5300		Logatchev, MAR	
32	100-300		100-300	700-5200				300-3100	100-700 Ni	Rainbow vent field, MAR	Marques et al. (2006)
2	<200-200	<200-400	<200	1050		<200	<200	1550	<200 Ni	Kairei vent field, Indian Ridge	Wang et al. (2014)
7	264	326	49	1390		124	64	3237	1400-2000 Se Avg 151 Au Avg 13 Se	Longqi, Southwest Indian Ridge	(Zhang et al., 2018)
	400-900		100-700					3800-7100		Southern JDFR	Paradis et al. (1988)
									Chalcocite (Cu_2S)		
15		43.5					17.8		4.92 Au, 87.9 Se, 4.4 Te	Logatchev, MAR	Wohlgemuth-Ueberwasser et al. (2015)
5		749					304		4.16 Au, bdl Se, 0.69 Te	Satanic Mills, Pacmanus, PNG	Wohlgemuth-Ueberwasser et al. (2015)
									Bornite (Cu_5FeS_4)		
3	1700	<400				<1400	<600			Pacmanus Chimney, PNG	Binns and Scott (1993)
11	230	9.97	5.56	0.06		84.4	4.57	200	0.826 Au	Wocan hydrothermal field, Carlsberg	Wang et al. (2017)

No.	Ag	As	Cd	Co	Cu	Pb	Sb	Zn	Other	Location (setting)	Authors
									9.24 Ge	Ridge, Indian Ocean	
									Chalcocite-Covellite (Cu_2S-CuS)		
12		6.75					1.38		0.55 Au, 7.3 Te	Logatchev, MAR	Wohlgemuth-Ueberwasser et al. (2015)
14		100				bdl	100	100		Logatchev, MAR	
									Covellite (CuS)		
3	0-700	0-3700	0-300	0-500			0-10	0-400	Au, 100 In, 6-300 Mn	Menez Gwen Field, MAR	Lein et al. (2010)
									1-300 Mn		
8	<200	<200	<200	<200-200		<200	<200	<200	<200-200 Ni	Kairei vent field, Indian Ridge	Wang et al. (2014)
									<200-500 Se		
2	1050	<200					200	1100	150 Hg, <200 Se	Hook Ridge, Antarctica	Petersen et al. (2004)
									Digenite (Cu_9S_5)		
9	<200	<200	<200	<200		<200	<200	<200	<200 Ni, <200 Se	Kairei vent field, Indian Ridge	Wang et al. (2014)
11	350	17.7	5.39	0.08		77.5	3.12	b.d.l.	Avg 41000 Fe	Wocan hydrothermal field, Carlsberg	Wang et al. (2017)
									5.45 Ga, 4.78 Ge	Ridge, Indian Ocean	
									Enargite (Cu_3AsS_4)		
10	500						300	9400	5200 Fe, 300 Hg, 1000 Se	Hook Ridge, Antarctica	Petersen et al. (2004)
30	2800		<200			13100	13300	17800	12400 Fe, 5100 Hg	Palinuro Volcanic Complex, Aeolian Arc, Italy	Petersen et al. (2014)
3						700-14600	0-700	3300-15800	2700-8400 Fe	Hakurei Deposit, Bayonnaise Knoll, Uzu-Bonin-Arc	Watanabe and Hayashi (2014)
25	200-7400		0-100				200-2400		100-3500 Fe	Yonaguni Knoll, Okinawa Trough	Suzuki et al. (2008)
									100-700 Mn, 200-500 Mo		
									Tennantite/Tetrahedrite ($Cu_{12}As_4S_{13}$-$Cu_{12}Sb_4S_{13}$)		
38	8000	178500				4500	20900	88500	3800 Fe, 1000 Hg, 900 Se	Hook Ridge, Antarctica	Petersen et al. (2004)
368	2700	40400	<200			<2000	241800	24000	42100 Fe, 4400 Hg	Palinuro Volcanic Complex, Aeolian Arc, Italy	Petersen et al. (2014)
	1600-3600	166300-198400					0-34500	72800-96400	7200-7700 Fe	Hakurei Deposit, Bayonnaise Knoll, Uzu-Bonin-Arc	Watanabe and Hayashi (2014)
8	10000-73250	56500-124500					17250-145000	55000-67750	2000-6000 Fe	Central Okinawa Trough	Halbach et al. (1993)
5	74600	71120				2320	167440	61640	11080 Fe, 1140 Mn	North Knoll, Iheya Ridge, Okinawa Trough	Ueno et al. (2003)
28	1800-33600	99500-133500	0-200				200-33800	51000-59600	5500-8000 Fe, 400-15300 Mn	Yonaguni Knoll, Okinawa Trough	Suzuki et al. (2008)
7	1100-1600	188000-191000				3500-6900	900-1200	25000-47000	46000-64000 Fe	Pacmanus Chimney, PNG	Binns and Scott (1993)

No.	Ag	As	Cd	Co	Cu	Pb	Sb	Zn	Other	Location (setting)	Authors
7		81298					3609		15.9 Au, <5 Se, 0.5 Te	Satanic Mills, Pacmanus, PNG	Wohlgemuth-Ueberwasser et al. (2015)
5		198500				750	5650	18550	61850 Fe	Satanic Mills, Pacmanus, PNG	
24	100	<200	1100		1800		<200	3400	Galena (PbS) <200 Fe, <200 Ga, <200 Hg <200 Se	Hook Ridge, Antarctica	Petersen et al. (2004)
36	500	<1000	800		300		9400	2300	300 Fe, 200 Hg	Palinuro Volcanic Complex, Aeolian Arc, Italy	Petersen et al. (2014)
3	1266.6				966.6		1100			Alice Spring Field, Mariana Trough	Iwaida and Ueno (2005)
5	2160				320		2740			North Knoll, Iheya Ridge, Okinawa Trough	Ueno et al. (2003)
83	200-1800				700-7700					Yonaguni Knoll, Okinawa Trough	Suzuki et al. (2008)
7	600							2000	4416 Fe, 557 Se	Endeavour Segment, JDFR	Tivey et al. (1999)